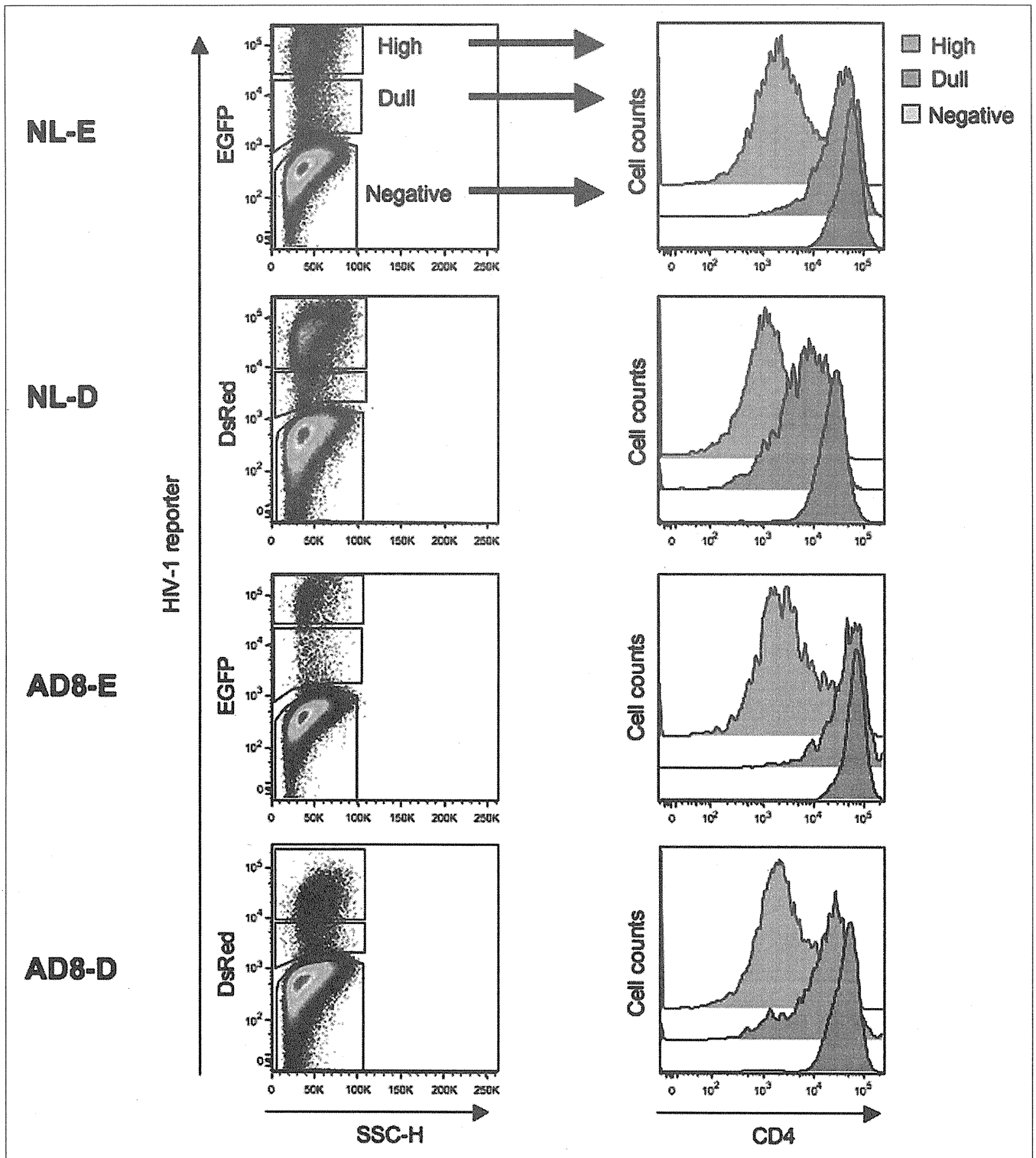

FIGURE 2 | Flow cytometry analysis of HIV-1-infected cells. Unstimulated CD4+ T cells were infected with HIV-1_{NL-E}, HIV-1_{NL-D}, HIV-$1_{NLAD8-E}$, or HIV-$1_{NLAD8-D}$ and cultured for 5 days (including the initial 1 day culture with TCR-stimulation). (Left panels) representative pseudo-color plot profiles for the $Dead^-/CD3^+/CD8^-$-gated cell fractions from three donors. Cells were classified as high (red), dull (blue), and negative (black) based on the HIV-1 reporter intensity. (Right panels) histograms of CD4 expression by the high (red), dull (blue), and negative (black) fractions defined.

T cells from three donors were infected with HIV-1_{NL-E} followed by TCR-stimulation for 1 day and cultivation for a further 4 days. **Figure 5A** shows a representative flow cytometric analysis. At 1 day post-infection, 17.6% of Gag $p24^+$ cells were observed,

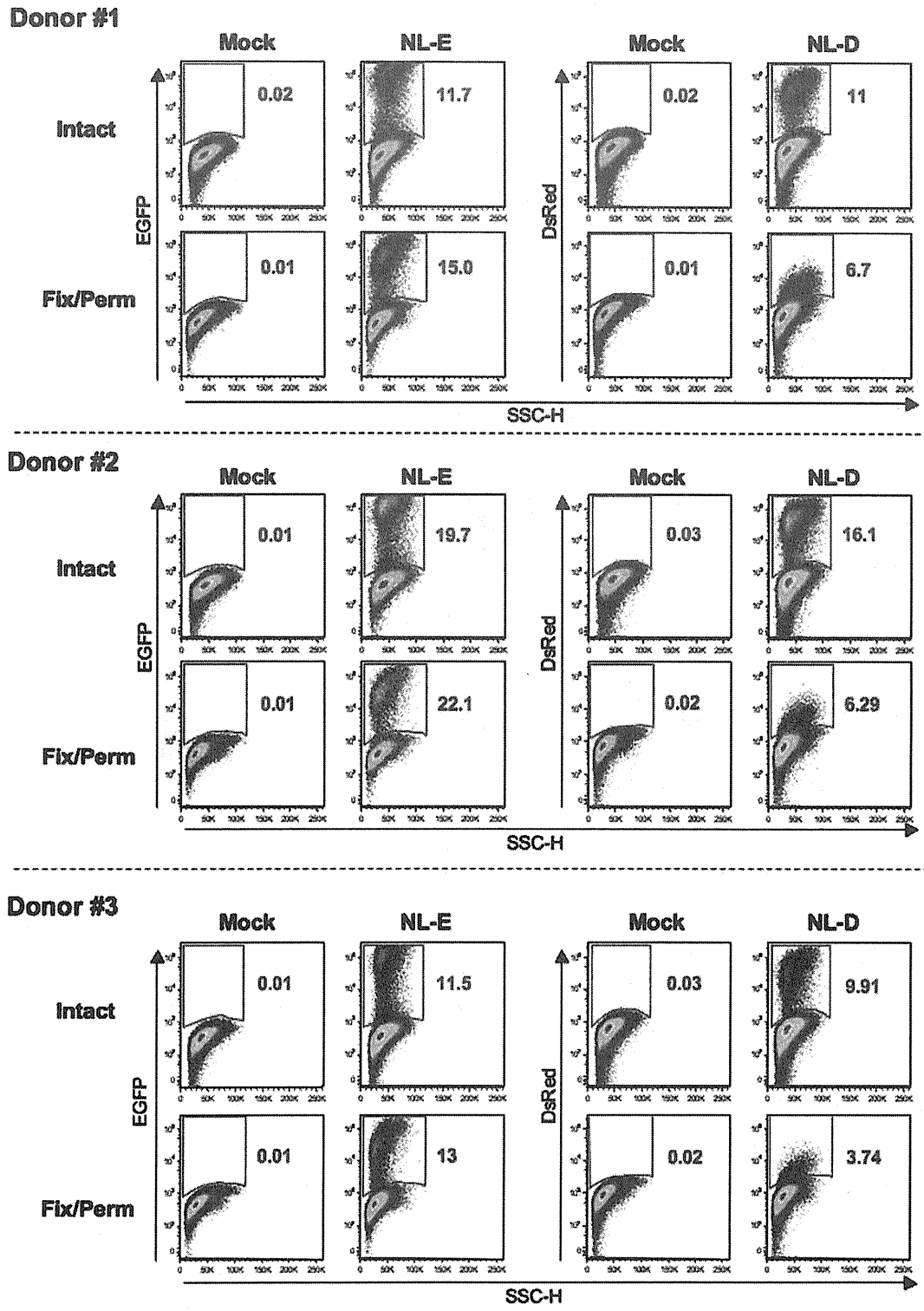

FIGURE 3 | Influence of fixation/permeabilization treatment on HIV-1 fluorescent reporter signals. Pseudo-color plot profiles for the Dead$^-$/CD3$^+$/CD8$^-$-gated cell fractions from the mock, HIV-1$_{NL-E}$ infection (NL-E), and HIV-1$_{NL-D}$ infection (NL-D) groups from all three donors tested. Analyzed cells were prepared as outlined in the legend to **Figure 2** and then either fixed/permeabilized (fix/perm) or not (intact).

despite the fact that no EGFP$^+$ cells were detected. At 2 days post-infection, the proportion of EGFP$^-$Gag$^+$ cells was decreased and EGFP$^+$ cells including Gag p24$^+$ and Gag p24$^-$ cells became to be observed, suggesting that initially infecting HIV-1 was

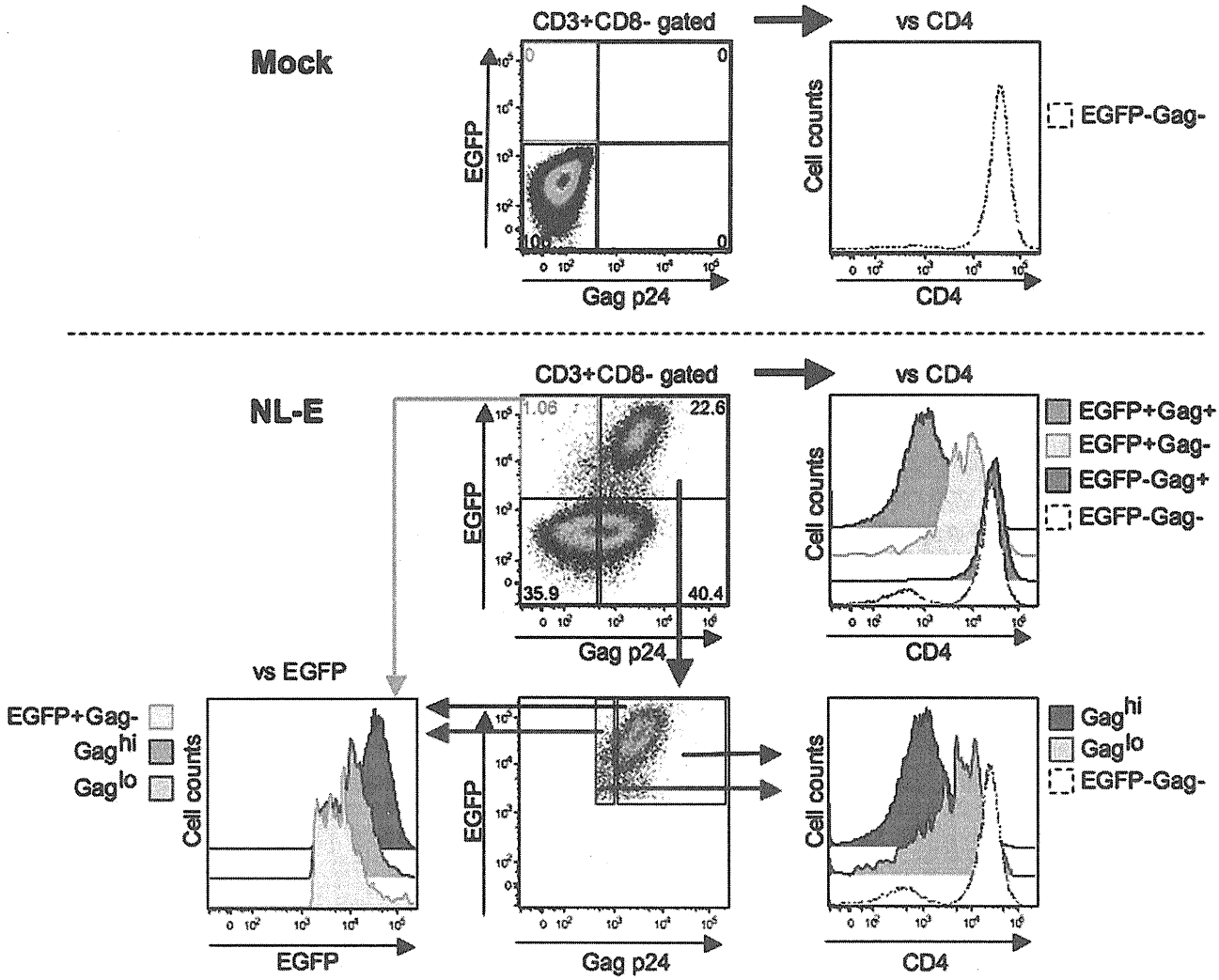

FIGURE 4 | Correlation between HIV-1 fluorescent reporter signal and Gag p24 expression. Representative flow cytometric analyses of the mock and HIV-1_{NL-E} infection groups from six donors. These infection groups were prepared as outlined in the legend to **Figure 2**. The $EGFP^+Gag^+$ (red), $EGFP^+Gag^-$ (green), $EGFP^-Gag^+$ (blue), $EGFP^-Gag^-$ (black), Gag^{hi} (brown), and Gag^{lo} (pink) cell fractions were categorized based on the expression patterns of EGFP and Gag p24. The expression levels of CD4 and EGFP in each cell fraction were compared according to their histogram profiles.

degraded and/or replaced with replication-competent proviruses. After 3 days post-infection, $EGFP^+$ cells were clearly visible and the proportion of $EGFP^-Gag^+$ cells turned to be increased, suggesting that progeny virus infection occurred. Because the CD4 expression levels were identical between $EGFP^-Gag^+$ cells and $EGFP^-Gag^-$ cells throughout the culture period, Gag p24 ICS must have detected cells that had bound or internalized HIV-1.

CEM–CCR5 cells, which are almost as susceptible to X4 and R5 HIV-1 fusion (data not shown), were used to confirm that Gag p24 ICS did indeed detect HIV-1-bound cells. Also, because it has been suggested that spinoculation at 25°C may induce HIV-1 fusion to the targeted cells (Dai et al., 2009), we tested Gag p24 ICS using CEM–CCR5 cells immediately after spinoculation with X4-tropic HIV-1_{NL-E} or R5-tropic HIV-1_{AD8-E} at 4°C. When cells were not fixed/permeabilized, no Gag $p24^+$ cells were detected by flow cytometry (**Figure 5B**, upper panels); however, when cells were fixed/permeabilized, a substantial proportion of Gag^+ cells was detectable in both the HIV-1_{NL-E} and HIV-1_{AD8-E} infection groups (**Figure 5B**, lower panels). Taken together, these results indicate that cells that have bound or internalized HIV-1 can be detected using flow cytometry for Gag p24 ICS.

THE INTENSITY OF THE HIV-1 FLUORESCENT REPORTER SIGNAL DEPENDS ON TCR-MEDIATED ACTIVATION LEVELS

T cell receptors-mediated activation of HIV-1-infected $CD4^+$ T cells increased productive viral replication, although the signaling pathway responsible may be different for X4 and R5 HIV-1 (Popik and Pitha, 2000). We investigated whether the intensity of the HIV-1 fluorescent reporter signal was affected by TCR-mediated

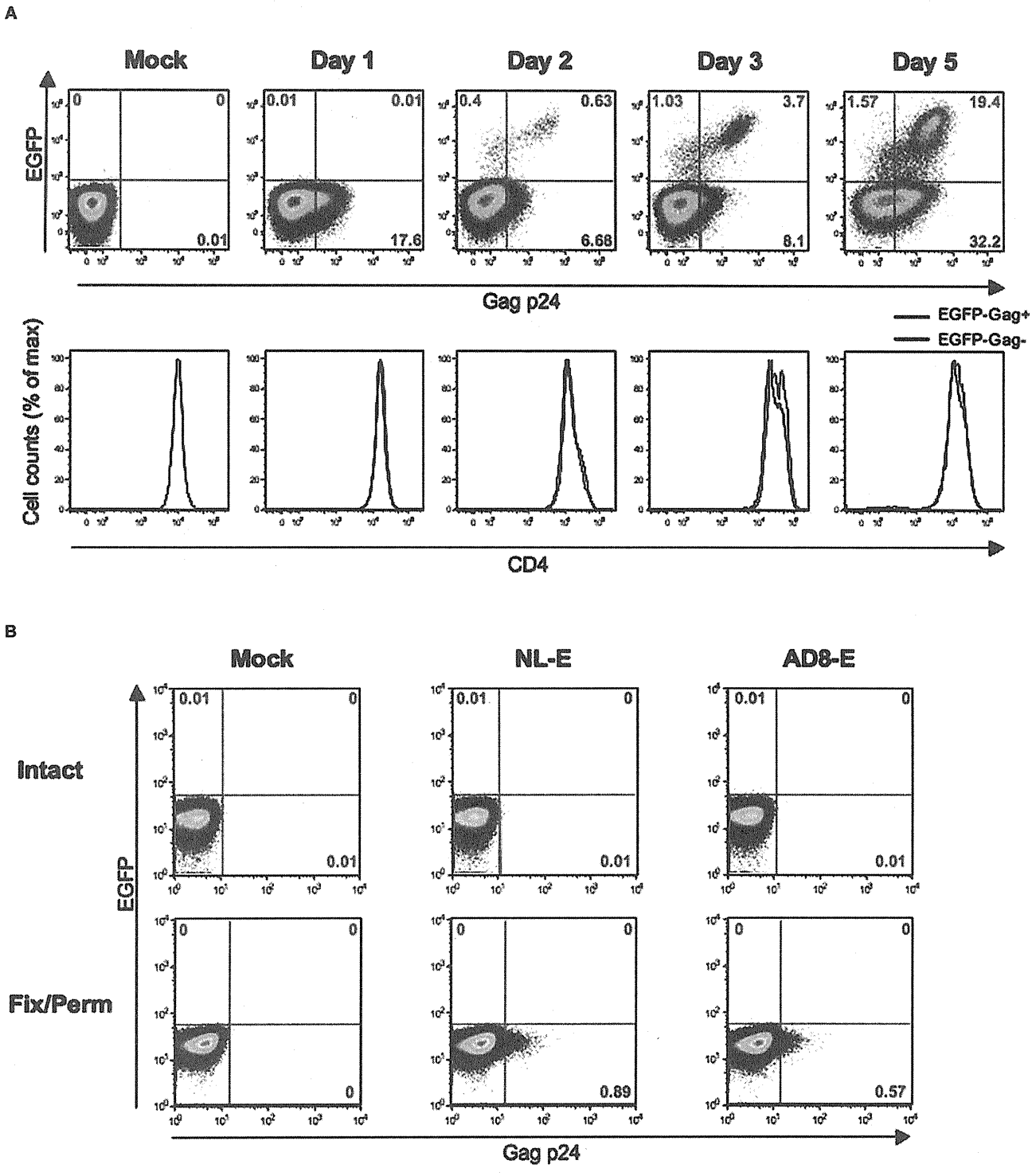

FIGURE 5 | Evaluation of Gag p24 ICS for HIV-1-internalized and -bound cells. (A) Representative flow cytometric analyses of the HIV-1_{NL-E} infection (NL-E) and mock (Mock) groups from three donors in which unstimulated primary $CD4^+$ T cells were infected with HIV-1_{NL-E} or not, respectively, and cultured for 5 days (including the initial 1 day culture with TCR-stimulation). The expression patterns of EGFP and Gag p24 are indicated in the pseudo-color plot profiles for the $Dead^-/CD3^+/CD8^-$-gated cell fractions (upper panels). The expression level of CD4 in $EGFP^-Gag^+$ and $EGFP^-Gag^-$ cells is indicated in the histograms by the blue and black lines, respectively (lower panels). **(B)** Representative flow cytometric analyses of Gag p24 staining. CEM–CCR5 cells were infected with HIV-1_{NL-E} (NL-E), HIV-1_{AD8-E} (AD8-E), or not (Mock). Immediately after spinoculation at 4°C, the cells were washed and fixed/permeabilized (fix/perm) or not (intact) prior to Gag p24 staining.

activation levels. In this experiment, primary $CD4^+$ T cells from four donors were individually pre-stimulated via the TCR for 4 (weak stimulation) or 24 h (strong stimulation), infected with HIV-$1_{NL\text{-}E}$, and then cultured for a further 3 days. First, we confirmed that this experimental protocol allowed the preferential production of HIV-$1_{NL\text{-}E}$ upon strong stimulation in all donors by examining the cell culture supernatants by ELISA (**Figure 6A**) and real-time RT-PCR (**Figure 6B**). Flow cytometric analysis of intact cells showed that HIV-$1_{NL\text{-}E}^+$ ($EGFP^+$) cells were more prevalent after strong stimulation than after weak stimulation, although the proportion of HIV-$1_{NL\text{-}E}^+$ cells varied among individuals (**Figure 6C**, upper and middle panels). The PMT voltage was optimized for EGFP to prevent excessive EGFP signaling (**Figures 2** and **3**). Of note, EGFP expression by HIV-$1_{NL\text{-}E}^+$ cells was lower in the weak stimulation group than in the strong stimulation group (as observed in donors #4 and #5), and EGFP expression in the weak stimulation group approached that in the strong stimulation group in parallel with the increase in the number of HIV-$1_{NL\text{-}E}^+$ cells (as observed in donors #6 and #7; **Figure 6C**, lower panels). Taken together, these results show that the intensity of the fluorescent reporter is highly correlated with the viral replication level.

DISCUSSION

Flow cytometric analysis is a reliable and convenient method for detecting HIV-1-infected cells at a single cell level. Here, we studied the potential usefulness of several HIV-1 fluorescent reporters that have been published previously (Yamamoto et al., 2009). We examined whether they would be helpful for evaluating viral replication levels based on their fluorescence intensity. In this study, we used recombinant HIV-1 encoding either EGFP or DsRed to show that the fluorescence intensity of the EGFP and DsRed reporters was associated with the level of CD4 downmodulation (**Figure 2**). Furthermore, we showed that EGFP intensity was associated with the expression level of Gag p24 (**Figure 4**). These findings clearly indicate that fluorescent reporter intensity is useful for evaluating viral replication levels. To confirm this argument, we further compared the fluorescent reporter intensity of HIV-1-infected cells that were strongly or weakly stimulated via the TCR. As expected, higher levels of HIV-1 replication/production occurred in strongly stimulated cells from all the donors tested (**Figure 6A,B**). Although the proportion and EGFP intensity of the HIV-1-infected cells varied among individuals, this might be due to differing susceptibility to HIV-1 and/or TCR-stimulation. Thus, the variability in EGFP expression is rather favorable to our argument, as increased EGFP intensity was associated with an increase in the number of HIV-1-infected cells after weak stimulation (**Figure 6C**).

Although Gag p24 ICS is usually used for flow cytometric analysis of other markers, we showed that it can also be used to detect cells that have internalized or bound HIV-1 (**Figure 5A,B**). However, Gag p24 ICS did not appear sensitive enough to detect HIV-1-infected cells because some HIV-1-infected cells in which CD4 was moderately downmodulated were identified as positive for EGFP but negative for Gag p24 (**Figure 4**). Bosque and Planelles (2009) also identified a small population of such reporter-positive but Gag p24-negative cells by flow cytometry when $CD4^+$ T cells were infected with EGFP-encoded DHIV incorporating a small out-of-frame deletion in the gp120-encoding area and pseudotyped with X4-tropic HIV-1_{LAI}, and assumed that these cells were at an early stage of the infection process and did not display late viral proteins. Therefore, our own findings indicate that it is the HIV-1 fluorescent reporter, rather than Gag p24 staining, that reliably detects HIV-1-infected cells at different stages of infection in flow cytometry experiments.

It is known that maturation of DsRed for coloration is usually slower compared with EGFP (Bevis and Glick, 2002; Maruyama et al., 2004). When we focused on the HIV-1 dull fraction in **Figure 2**, we found that CD4 downmodulation was stronger in $DsRed^+$ cells than in $EGFP^+$ cells. These results suggest that the EGFP reporter is preferable to the DsRed reporter for detection of earlier stage of infection. Furthermore, the detrimental effect of fixation/permeabilization on fluorescent reporter intensity, particularly when using the DsRed reporter, should be noted (**Figure 3**). Although the detailed mechanism remains obscure, this may result from the lower fluorescence intensity of DsRed compared with EGFP. A similar phenomenon was described regarding fixation with 3% paraformaldehyde, which significantly decreases the fluorescence intensity of DsRed, although specific data were not provided (Weber et al., 2006). Regardless of the weakened signal, the EGFP reporter is still compatible with fixation/permeabilization because the proportion of $EGFP^+$ cells was comparable between intact cells and fixated/permeabilized cells (**Figure 3**). Therefore, the EGFP reporter still maintains an advantage for analyses of cytokine/chemokine production and proliferation assays based on Ki-67 expression, for which ICS is necessary.

The HIV-1 fluorescent reporter has a potential application in molecular biology. In general, ICS-treated cells are not suitable for analysis using molecular biology techniques, since formaldehyde-based fixation (required for ICS) makes RNA extraction and reverse transcription and quantification problematic (Farragher et al., 2008) because of chemical cross-linking of proteins and nucleic acids (Kuykendall and Bogdanffy, 1992; Finke et al., 1993; Park et al., 1996), degradation of RNA (Bresters et al., 1994), and covalent modification of RNA via the addition of monomethylol groups to the bases (Masuda et al., 1999); therefore, by using the HIV-1 fluorescent reporter, HIV-1-infected cells can be sorted/purified without the need for fixation, allowing further characterization at a molecular level.

Given the usefulness of the HIV-1 fluorescent reporter shown here, it would also be very useful for investigating the mechanisms involved in the selective replication of R5 HIV-1 over X4 HIV-1 during the acute phase *in vivo* (Wolinsky et al., 1992; Zhu et al., 1993; van't Wout et al., 1994) and in cell culture systems *in vitro* (Schweighardt et al., 2004; Roy et al., 2005). We previously developed an *in vitro* dual infection model using EGFP-encoded X4 HIV-1 (HIV-$1_{NL\text{-}E}$) and DsRed-encoded R5 HIV-1 (HIV-$1_{AD8\text{-}D}$) and showed that the increase in the proportion of X4 HIV-1-infected cells is dependent upon their activation level (Yamamoto et al., 2009). Furthermore, the results of the present study show that the fluorescence intensity of the reporter molecule

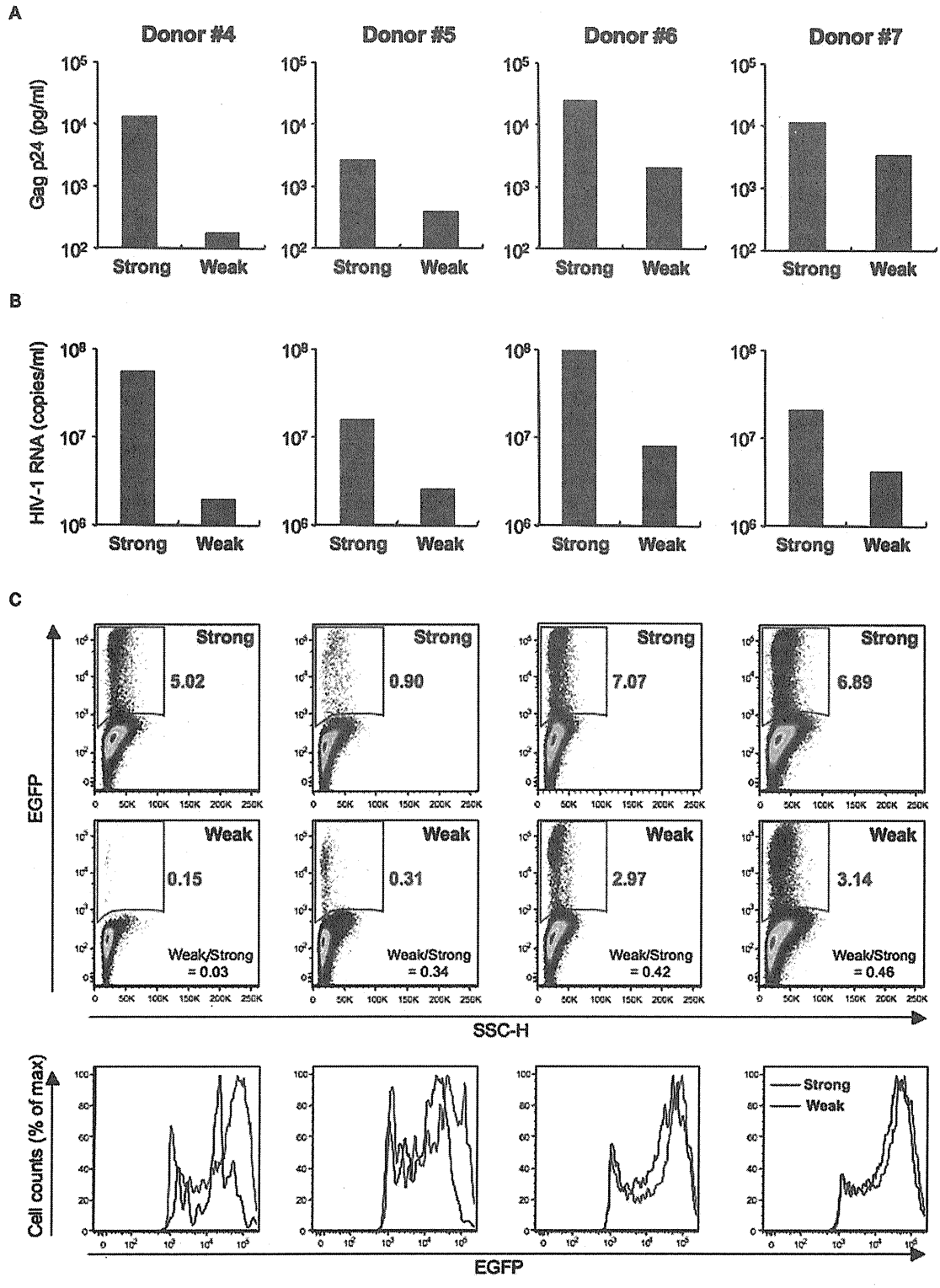

FIGURE 6 | Differences of HIV-1 replication according to TCR-mediated activation levels. Primary CD4$^+$ T cells from four donors (Donor #4–7) were pre-stimulated via TCR for 4 (Weak; blue) or 24 h (Strong; red) and then infected with HIV-1_{NL-E} and cultured for 3 days. **(A)** ELISA for HIV-1 Gag p24 in the culture supernatants. **(B)** Quantitative real-time RT-PCR for HIV-1 RNA in the culture supernatants. **(C)** Flow cytometric analysis of intact cells showing pseudo-color plot profiles (Dead$^-$/CD3$^+$/CD8$^-$-gated cell fraction; upper and middle panels) and histogram profiles (Dead$^-$/CD3$^+$/CD8$^-$/EGFP$^+$-gated cell fraction; lower panels).

can be used to assess the level of viral replication in infected cells; therefore, by focusing on the HIV-1-infected cells and the fluorescent reporter intensity in the dual infection model, the detailed mechanism(s) of HIV-1 infection/pathogenesis can be clarified. In this regard, we have been investigating the dynamics of HIV-1 infection *in vivo* using humanized mice infected simultaneously with EGFP-encoded X4 HIV-1 (HIV-1_{NL-E}) and DsRed-encoded R5 HIV-1 (HIV-1_{AD8-D}; Ishige et al., in preparation). We believe that the advantages of the recombinant HIV-1 fluorescent reporter will contribute to the further understanding of HIV-1 infection/pathogenesis.

ACKNOWLEDGMENTS

We thank Kaori Okano for technical support. This work was supported in part by Grants from the Ministry of Education, Science, Sports, and Culture of Japan (Kazutaka Terahara), and the Ministry of Health, Labour, and Welfare of Japan (Kazutaka Terahara and Yasuko Tsunetsugu-Yokota).

REFERENCES

Berger, E. A., Murphy, P. M., and Farber, J. M. (1999). Chemokine receptors as HIV-1 coreceptors: roles in viral entry, tropism, and disease. *Annu. Rev. Immunol.* 17, 657–700.

Bevis, B. J., and Glick, B. S. (2002). Rapidly maturing variants of the Discosoma red fluorescent protein (DsRed). *Nat. Biotechnol.* 20, 83–87.

Bosque, A., and Planelles, V. (2009). Induction of HIV-1 latency and reactivation in primary memory $CD4^+$ T cells. *Blood* 113, 58–65.

Bresters, D., Schipper, M. E., Reesink, H. W., Boeser-Nunnink, B. D., and Cuypers, H. T. (1994). The duration of fixation influences the yield of HCV cDNA-PCR products from formalin-fixed, paraffin-embedded liver tissue. *J. Virol. Methods* 48, 267–272.

Chalfie, M. (1995). Green fluorescent protein. *Photochem. Photobiol.* 62, 651–656.

Cubitt, A. B., Heim, R., Adams, S. R., Boyd, A. E., Gross, L. A., and Tsien, R. Y. (1995). Understanding, improving and using green fluorescent proteins. *Trends Biochem. Sci.* 20, 448–455.

Dai, J., Agosto, L. M., Baytop, C., Yu, J. J., Pace, M. J., Liszewski, M. K., and O'doherty, U. (2009). Human immunodeficiency virus integrates directly into naive resting $CD4^+$ T cells but enters naive cells less efficiently than memory cells. *J. Virol.* 83, 4528–4537.

Dorsky, D. I., Wells, M., and Harrington, R. D. (1996). Detection of HIV-1 infection with a green fluorescent protein reporter system. *J. Acquir. Immune Defic. Syndr. Hum. Retrovirol.* 13, 308–313.

Farragher, S. M., Tanney, A., Kennedy, R. D., and Paul Harkin, D. (2008). RNA expression analysis from formalin fixed paraffin embedded tissues. *Histochem. Cell Biol.* 130, 435–445.

Finke, J., Fritzen, R., Ternes, P., Lange, W., and Dolken, G. (1993). An improved strategy and a useful housekeeping gene for RNA analysis from formalin-fixed, paraffin-embedded tissues by PCR. *Biotechniques* 14, 448–453.

Gervaix, A., West, D., Leoni, L. M., Richman, D. D., Wong-Staal, F., and Corbeil, J. (1997). A new reporter cell line to monitor HIV infection and drug susceptibility in vitro. *Proc. Natl. Acad. Sci. U.S.A.* 94, 4653–4658.

Heim, R., Cubitt, A. B., and Tsien, R. Y. (1995). Improved green fluorescence. *Nature* 373, 663–664.

Kar-Roy, A., Dong, W., Michael, N., and Li, Y. (2000). Green fluorescence protein as a transcriptional reporter for the long terminal repeats of the human immunodeficiency virus type 1. *J. Virol. Methods* 84, 127–138.

Kuykendall, J. R., and Bogdanffy, M. S. (1992). Efficiency of DNA-histone crosslinking induced by saturated and unsaturated aldehydes in vitro. *Mutat. Res.* 283, 131–136.

Malim, M. H., and Emerman, M. (2008). HIV-1 accessory proteins – ensuring viral survival in a hostile environment. *Cell Host Microbe* 3, 388–398.

Maruyama, M., Nishio, T., Yoshida, T., Ishida, C., Ishida, K., Watanabe, Y., Nishikawa, M., and Takakura, Y. (2004). Simultaneous detection of DsRed2-tagged and EGFP-tagged human beta-interferons in the same single cells. *J. Cell. Biochem.* 93, 497–502.

Masuda, N., Ohnishi, T., Kawamoto, S., Monden, M., and Okubo, K. (1999). Analysis of chemical modification of RNA from formalin-fixed samples and optimization of molecular biology applications for such samples. *Nucleic Acids Res.* 27, 4436–4443.

Mcclure, M. O., Sattentau, Q. J., Beverley, P. C., Hearn, J. P., Fitzgerald, A. K., Zuckerman, A. J., and Weiss, R. A. (1987). HIV infection of primate lymphocytes and conservation of the CD4 receptor. *Nature* 330, 487–489.

O'doherty, U., Swiggard, W. J., and Malim, M. H. (2000). Human immunodeficiency virus type 1 spinoculation enhances infection through virus binding. *J. Virol.* 74, 10074–10080.

Page, K. A., Liegler, T., and Feinberg, M. B. (1997). Use of a green fluorescent protein as a marker for human immunodeficiency virus type 1 infection. *AIDS Res. Hum. Retroviruses* 13, 1077–1081.

Park, Y. N., Abe, K., Li, H., Hsuih, T., Thung, S. N., and Zhang, D. Y. (1996). Detection of hepatitis C virus RNA using ligation-dependent polymerase chain reaction in formalin-fixed, paraffin-embedded liver tissues. *Am. J. Pathol.* 149, 1485–1491.

Popik, W., and Pitha, P. M. (2000). Inhibition of CD3/CD28-mediated activation of the MEK/ERK signaling pathway represses replication of X4 but not R5 human immunodeficiency virus type 1 in peripheral blood CD4(+) T lymphocytes. *J. Virol.* 74, 2558–2566.

Roy, A. M., Schweighardt, B., Eckstein, L. A., Goldsmith, M. A., and Mccune, J. M. (2005). Enhanced replication of R5 HIV-1 over X4 HIV-1 in CD4(+)CCR5(+)CXCR4(+) T cells. *J. Acquir. Immune Defic. Syndr.* 40, 267–275.

Saito, A., Nomaguchi, M., Iijima, S., Kuroishi, A., Yoshida, T., Lee, Y. J., Hayakawa, T., Kono, K., Nakayama, E. E., Shioda, T., Yasutomi, Y., Adachi, A., Matano, T., and Akari, H. (2010). Improved capacity of a monkey-tropic HIV-1 derivative to replicate in cynomolgus monkeys with minimal modifications. *Microbes Infect.* 13, 58–64.

Schweighardt, B., Roy, A. M., Meiklejohn, D. A., Grace, E. J., 2nd, Moretto, W. J., Heymann, J. J., and Nixon, D. F. (2004). R5 human immunodeficiency virus type 1 (HIV-1) replicates more efficiently in primary $CD4^+$ T-cell cultures than X4 HIV-1. *J. Virol.* 78, 9164–9173.

Tsunetsugu-Yokota, Y. (2008). "Transmission of HIV from dendritic cells to $CD4^+$ T cells: a promising target for vaccination and therapeutic intervention," in *AIDS Vaccines, HIV Receptors and AIDS Research*, ed. L. B. Kendow (New York: Nova Science Publishers, Inc.), 117–128.

Tsunetsugu-Yokota, Y., Akagawa, K., Kimoto, H., Suzuki, K., Iwasaki, M., Yasuda, S., Hausser, G., Hultgren, C., Meyerhans, A., and Takemori, T. (1995). Monocyte-derived cultured dendritic cells are susceptible to human immunodeficiency virus infection and transmit virus to resting T cells in the process of nominal antigen presentation. *J. Virol.* 69, 4544–4547.

van't Wout, A. B., Kootstra, N. A., Mulder-Kampinga, G. A., Albrecht-Van Lent, N., Scherpbier, H. J., Veenstra, J., Boer, K., Coutinho, R. A., Miedema, F., and Schuitemaker, H. (1994). Macrophage-tropic variants initiate human immunodeficiency virus type 1 infection after sexual, parenteral, and vertical transmission. *J. Clin. Invest.* 94, 2060–2067.

Weber, J., Weberova, J., Carobene, M., Mirza, M., Martinez-Picado, J., Kazanjian, P., and Quinones-Mateu, M. E. (2006). Use of a novel assay based on intact recombinant viruses expressing green (EGFP) or red (DsRed2) fluorescent proteins to examine the contribution of pol and env genes to overall HIV-1 replicative fitness. *J. Virol. Methods* 136, 102–117.

Wolinsky, S. M., Wike, C. M., Korber, B. T., Hutto, C., Parks, W. P., Rosenblum, L. L., Kunstman, K. J., Furtado, M. R., and Munoz, J. L. (1992). Selective transmission of human immunodeficiency virus type-1 variants from mothers to infants. *Science* 255, 1134–1137.

Yamamoto, T., Tsunetsugu-Yokota, Y., Mitsuki, Y. Y., Mizukoshi, F., Tsuchiya, T., Terahara, K., Inagaki, Y., Yamamoto, N., Kobayashi, K., and Inoue, J. (2009). Selective transmission of R5 HIV-1 over X4 HIV-1 at the dendritic cell-T cell infectious synapse is determined by the T cell activation state. *PLoS Pathog.* 5, e1000279. doi:10.1371/journal.ppat.1000279

Zhu, T., Mo, H., Wang, N., Nam, D. S., Cao, Y., Koup, R. A., and Ho, D. D. (1993). Genotypic and phenotypic characterization of HIV-1 patients with primary infection. *Science* 261, 1179–1181.

Conflict of Interest Statement: The authors declare that the research was conducted in the absence of any commercial or financial relationships that could be construed as a potential conflict of interest.

Received: 29 November 2011; accepted: 28 December 2011; published online: 10 January 2012.
Citation: Terahara K, Yamamoto T, Mitsuki Y-y, Shibusawa K, Ishige M, Mizukoshi F, Kobayashi K and Tsunetsugu-Yokota Y (2012) Fluorescent reporter signals, EGFP, and DsRed, encoded in HIV-1 facilitate the detection of productively infected cells and cell-associated viral replication levels. Front. Microbio. 2:280. doi: 10.3389/fmicb.2011.00280
This article was submitted to Frontiers in Virology, a specialty of Frontiers in Microbiology.

OPEN ACCESS Freely available online

PLoS one

A Single Amino Acid of Human Immunodeficiency Virus Type 2 Capsid Protein Affects Conformation of Two External Loops and Viral Sensitivity to TRIM5α

Tadashi Miyamoto[1], Masaru Yokoyama[2], Ken Kono[1,3], Tatsuo Shioda[1], Hironori Sato[2], Emi E. Nakayama[1]*

1 Department of Viral infections, Research Institute for Microbial Diseases, Osaka University, Suita, Osaka, Japan, 2 Pathogen Genomics Center, National Institute of Infectious Diseases, Musashi Murayama, Tokyo, Japan, 3 Research Fellow of the Japan Society for the Promotion of Science, Tokyo, Japan

Abstract

We previously reported that human immunodeficiency virus type 2 (HIV-2) carrying alanine or glutamine but not proline at position 120 of the capsid protein (CA) could grow in the presence of anti-viral factor TRIM5α of cynomolgus monkey (CM). To elucidate details of the interaction between the CA and TRIM5α, we generated mutant HIV-2 viruses, each carrying one of the remaining 17 possible amino acid residues, and examined their sensitivity to CM TRIM5α-mediated restriction. Results showed that hydrophobic residues or those with ring structures were associated with sensitivity, while those with small side chains or amide groups conferred resistance. Molecular dynamics simulation study revealed a structural basis for the differential TRIM5α sensitivities. The mutations at position 120 in the loop between helices 6 and 7 (L6/7) affected conformation of the neighboring loop between helices 4 and 5 (L4/5), and sensitive viruses had a common L4/5 conformation. In addition, the common L4/5 structures of the sensitive viruses were associated with a decreased probability of hydrogen bond formation between the 97th aspartic acid in L4/5 and the 119th arginine in L6/7. When we introduced aspartic acid-to-alanine substitution at position 97 (D97A) of the resistant virus carrying glutamine at position 120 to disrupt hydrogen bond formation, the resultant virus became moderately sensitive. Interestingly, the virus carrying glutamic acid at position 120 showed resistance, while its predicted L4/5 conformation was similar to those of sensitive viruses. The D97A substitution failed to alter the resistance of this particular virus, indicating that the 120th amino acid residue itself is also involved in sensitivity regardless of the L4/5 conformation. These results suggested that a hydrogen bond between the L4/5 and L6/7 modulates the overall structure of the exposed surface of the CA, but the amino acid residue at position 120 is also directly involved in CM TRIM5α recognition.

Citation: Miyamoto T, Yokoyama M, Kono K, Shioda T, Sato H, et al. (2011) A Single Amino Acid of Human Immunodeficiency Virus Type 2 Capsid Protein Affects Conformation of Two External Loops and Viral Sensitivity to TRIM5α. PLoS ONE 6(7): e22779. doi:10.1371/journal.pone.0022779

Editor: Young-Min Lee, Chungbuk National University, Korea, Republic of

Received February 7, 2011; **Accepted** July 7, 2011; **Published** July 28, 2011

Funding: This work was supported by grants from the Health Science Foundation, the Ministry of Education, Culture, Sports, Science, and Technology, and the Ministry of Health, Labour and Welfare, Japan. The funders had no role in study design, data collection and analysis, decision to publish, or preparation of the manuscript.

Competing Interests: The authors have declared that no competing interests exist.

* E-mail: emien@biken.osaka-u.ac.jp

Introduction

Human immunodeficiency virus type 1 (HIV-1) infects humans and chimpanzees but not Old World Monkeys (OWM) such as Rhesus monkey (Rh) and cynomolgus monkey (CM). This is attributed to a barrier in the host cell. In 2004, the screening of a Rh cDNA library identified TRIM5α as one of cellular antiviral factors [1]. TRIM5 is a member of the tripartite motif family containing RING, B-box and coiled-coil domains [2]. The alpha isoform of TRIM5 has an additional C-terminal PRYSPRY (B30.2) domain. Several studies have shown that sequence variation in variable regions of the PRYSPRY domain among different monkey species affects species-specific retrovirus infection [3–11].

Rh and CM TRIM5αs restrict HIV-1 but not simian immunodeficiency virus isolated from macaque (SIVmac) [1,5], whereas African green monkey (AGM) TRIM5α inhibits both HIV-1 and SIVmac [5,12]. Human TRIM5α only weakly restricts HIV-1, but potently restricts N-tropic murine leukemia virus (N-MLV) [11,12].

Details of the molecular mechanism of retrovirus restriction by TRIM5α have been gradually elucidated by several groups. TRIM5α associates with the N-MLV capsid in detergent-stripped virions [13] or with an artificially constituted core structure composed of an HIV-1 capsid-nucleocapsid (CA-NC) fusion protein in a PRYSPRY domain-dependent manner [14], indicating that the target of TRIM5α is multimerized capsids. In addition, it was demonstrated that engagement of a restriction-sensitive retroviral core results in TRIM5α degradation by a proteasome-dependent pathway [15]. In the presence of proteasome inhibitors, virions complete reverse transcription and form functional pre-integration complexes, but 2-long terminal repeat circle formation and gene expression remain impaired [16,17]. Recently, we have reported that AGM TRIM5α restricted SIVmac mainly via the proteasome-dependent pathway, whereas HIV-1 and HIV-2 restriction by AGM TRIM5α was both proteasome-dependent and proteasome-independent [18].

HIV-2 and SIVmac have very similar genomes [19], but vary in their ability to grow in the presence of TRIM5α from various

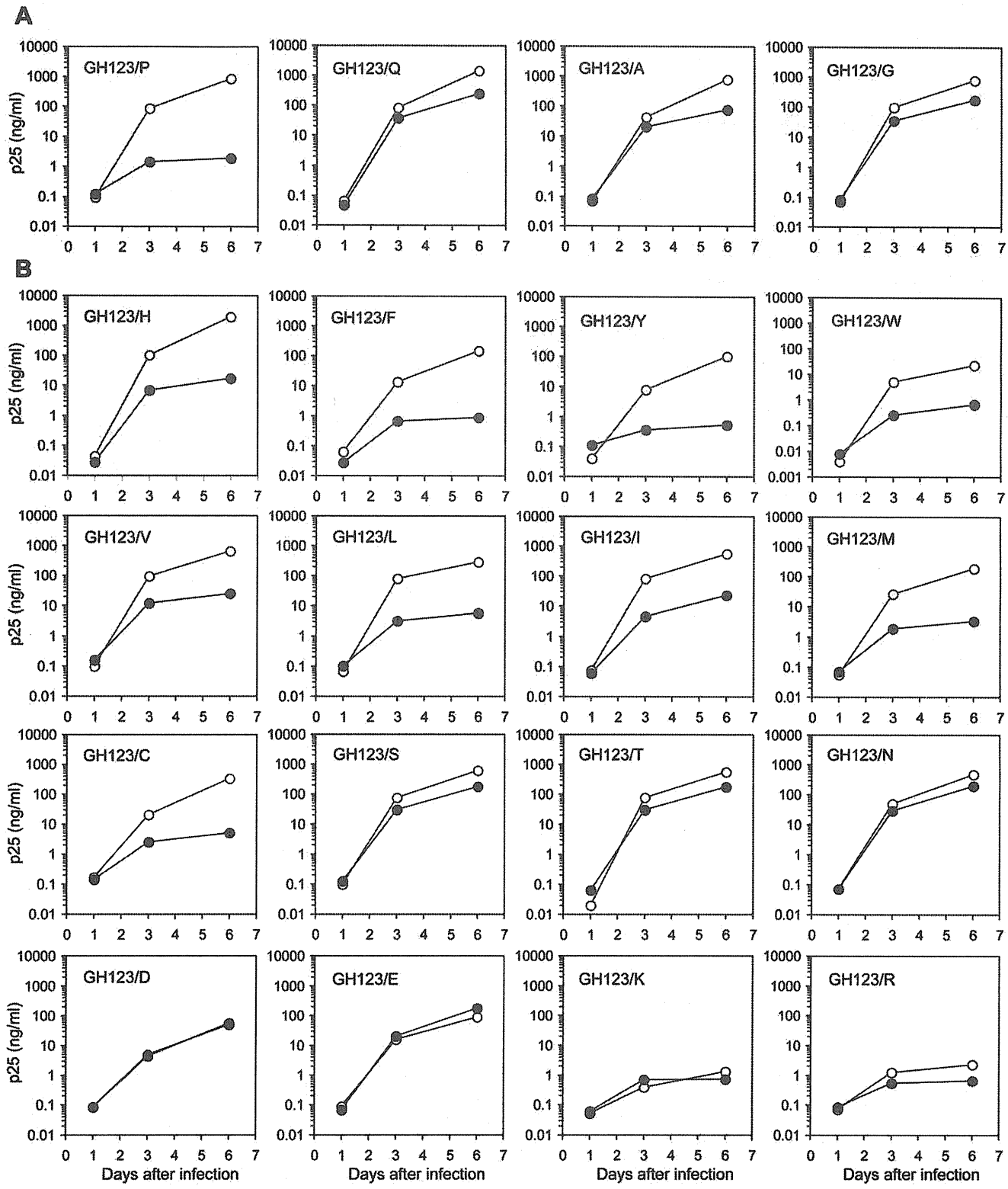

Figure 1. Growth of GH123 and its mutant viruses in the presence of CM TRIM5α. MT4 cells were infected with CM-TRIM5α-SeV (black circles) or CM-SPRY(–)-SeV (white circles) then superinfected with GH123 mutant viruses. Culture supernatants were periodically assayed for levels of virus capsid. Error bars show actual fluctuations between measurements of capsid in duplicate samples. A representative of two independent experiments is shown.
doi:10.1371/journal.pone.0022779.g001

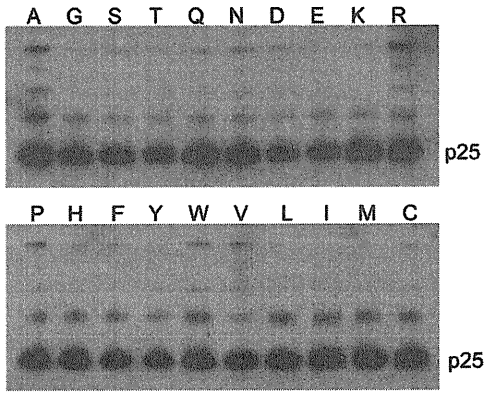

Figure 2. Western blot analysis of the CA in particles of GH123 and its mutant viruses. The viral particles of GH123 wild type and its mutant viruses were purified by ultracentrifugation through a 20% sucrose cushion. p25 capsid protein was visualized by western blotting (WB) using SIV-infected monkey serum.
doi:10.1371/journal.pone.0022779.g002

species. SIVmac239 is resistant to Rh and CM TRIM5αs [1,5,8], whereas HIV-2 strains GH123 and ROD are sensitive to these TRIM5αs [5,8,20,21]. We previously investigated the growth of eight different HIV-2 isolates in the presence of CM and human TRIM5αs and demonstrated that the growth of HIV-2 isolates carrying proline (P) at the 119th or 120th position of the capsid protein (CA) was inhibited by CM and human TRIM5αs, whereas the growth of those with either alanine (A) or glutamine (Q) was not affected by these TRIM5αs [20]. In a Caio cohort study in west Africa, it was demonstrated that subjects with a lower viral load more frequently carried a P at the 119th position of the CA, which corresponds to the 120th position of the GH123 CA, while non-proline residues at this position were more frequently observed in subjects with a high viral load [22], suggesting that TRIM5α controls viral replication in HIV-2-infected individuals.

The 120th amino acid is located in the loop between helices 6 and 7 (L6/7) [20]. Recently, we have succeeded in improving the replication of simian-tropic HIV-1 in CM cells by introducing the SIVmac L6/7 CA sequence [23]. In the present study, we generated mutant HIV-2 viruses each carrying one of the remaining 17 possible amino acid residues at the 120th position, and examined their susceptibilities to TRIM5α-mediated restriction in order to elucidate details of the interaction between HIV-2 CA and TRIM5α. Computer-assisted structural study showed that the mutations at position 120 in L6/7 affected conformation of the neighboring loop between helices 4 and 5 (L4/5).

Results

Amino acid residues at the 120th position of HIV-2 GH123 CA and viral susceptibility to CM TRIM5α

In a previous study, we reported that HIV-2 isolates carrying P at the 120th position of the CA were sensitive to CM and human TRIM5αs, whereas those with either A or Q were not [20]. In the Los Alamos sequence database, the amino acid residue at the 119th or 120th position of almost all HIV-2 CAs is P, A, Q or glycine (G). Therefore, we first generated mutant HIV-2 GH123 viruses carrying G at the 120th position (GH123/G) to investigate its effect on TRIM5α susceptibility.

Equal amounts of p25 of mutant and wild type viruses were inoculated into the human T cell line MT4 expressing CM TRIM5α, and culture supernatants were periodically assayed for CA production. In agreement with the results of the previous study, wild type GH123 carrying P at the 120th position (GH123/P) was sensitive to CM TRIM5α since this virus failed to grow in the presence of CM TRIM5α. On the other hand, GH123/G as well as GH123/Q (glutamine) and GH123/A (alanine) were

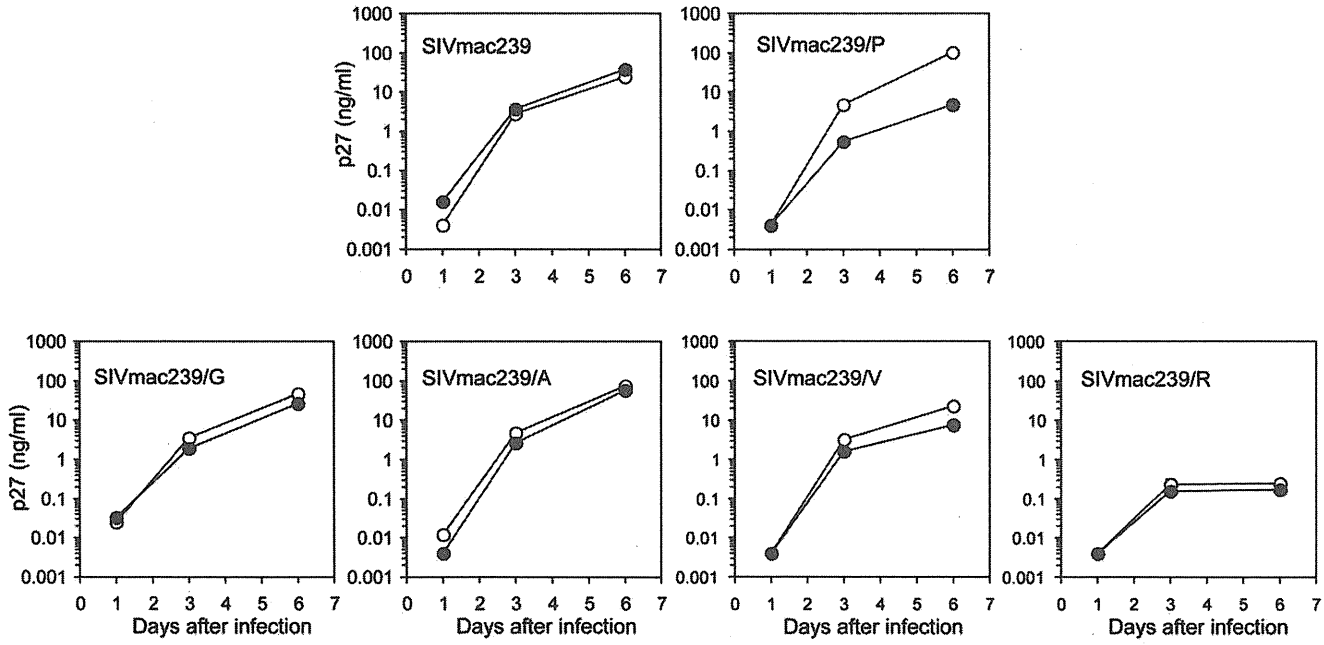

Figure 3. Growth of SIVmac239 and its mutant viruses in the presence of CM TRIM5α. MT4 cells were infected with CM-TRIM5α-SeV (black circles) or CM-SPRY(–)-SeV (white circles) then superinfected with SIVmac239 mutant viruses. Culture supernatants were periodically assayed for levels of virus capsid. Error bars show actual fluctuations between measurements of capsid in duplicate samples. A representative of three independent experiments is shown.
doi:10.1371/journal.pone.0022779.g003

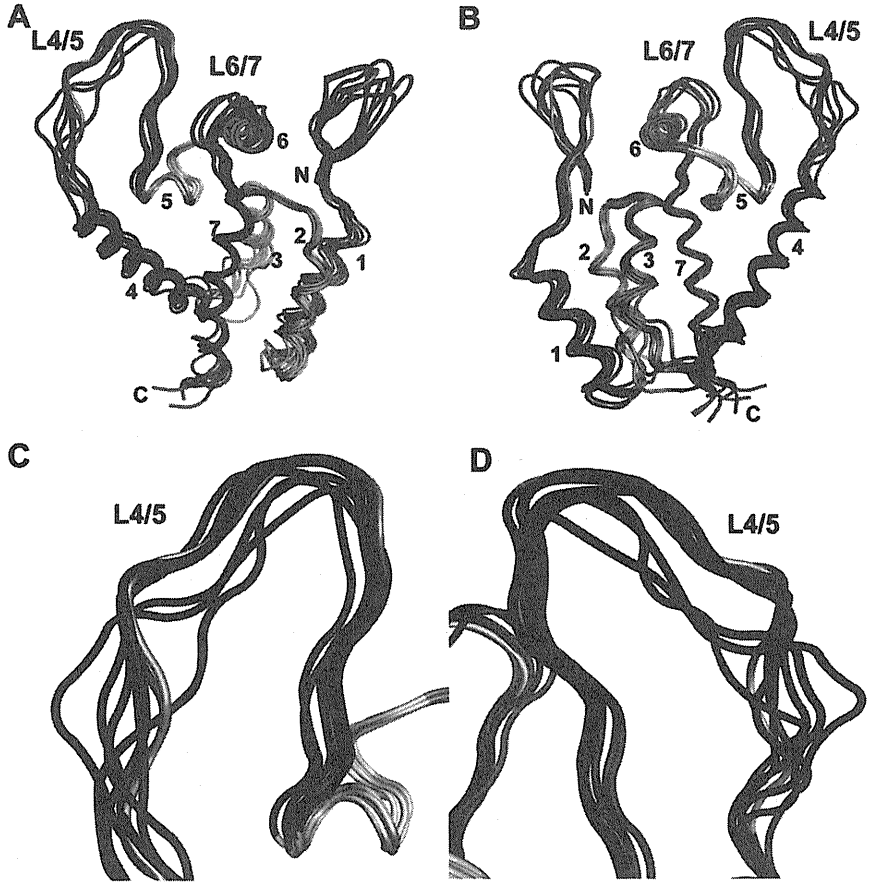

Figure 4. Structural models of the HIV-2 capsid N-terminal domain. Models were constructed by homology modeling and molecular dynamics simulations with the high-resolution X-ray crystal structure of the HIV-2 capsid N-terminal domain (PDB code: 2WLV [29]) as the starting structure. Averaged conformations of the overall structure of the N-terminal domain during 5–20 nanoseconds of MD simulations (A and B) and a close-up view around the L4/5 loop (C and D) are indicated. *N* and *C* indicate the amino termini and carboxyl termini, respectively; and the seven color-coded α-helices are labeled. Red and blue cartoons indicate the N-terminal loop, L4/5, and L6/7 of CM TRIM5α-sensitive (GH123/P, GH123/F, GH123/H and GH123/I) and CM TRIM5α-resistant (GH123/Q, GH123/A and GH123/N) viruses, respectively. Gray cartoons indicate the N-terminal loop, L4/5 and L6/7 of GH123/E in which the structures and biologic phenotypes are inconsistent. Models from two different angles are shown.
doi:10.1371/journal.pone.0022779.g004

resistant to CM TRIM5α, since these viruses could grow in the presence of CM TRIM5α (Figure 1A).

To determine whether amino acid residues other than P, Q, A and G can occupy the 120th position of HIV-2 GH123 CA, and to elucidate further details of the interaction between the CA and TRIM5α, we generated 16 mutant GH123 viruses each carrying one of the remaining possible amino acid residues at the 120th position. As shown in Figure 1B, viruses with amino acid residues bearing a ring structure including aromatic groups, namely, histidine (GH123/H), phenylalanine (GH123/F), tyrosine (GH123/Y), tryptophan (GH123/W) and GH123/P were all sensitive to CM TRIM5α. Hydrophobic valine (GH123/V), leucine (GH123/L), and isoleucine (GH123/I) viruses as well as sulfated methionine (GH123/M) and cysteine (GH123/C) viruses were also sensitive.

In contrast, viruses with amino acid residues bearing hydroxyl or amide groups, namely, serine (GH123/S), threonine (GH123/T), glutamine (GH123/Q) and asparagine (GH123/N) were resistant to CM TRIM5α. Acidic aspartic acid (GH123/D) and glutamic acid (GH123/E) viruses were also resistant, although they grew to slightly lower titers than wild type GH123/P in the absence of CM TRIM5α. The replication of viruses with basic arginine (GH123/R) and lysine (GH123/K) was severely impaired and it was impossible to evaluate the effects of these residues on susceptibility to TRIM5α. Almost identical results were obtained when we inoculated equal amounts of reverse transcriptase of mutant and wild type GH123 (data not shown). Thus, the nature of the 120th amino acid residue greatly affects viral sensitivity to CM TRIM5α.

CA processing is not affected by the 120th mutation

To understand why GH123/R and GH123/K failed to replicate even in the absence of TRIM5α, we examined the Gag processing of mutant and wild type HIV-2 GH123 viruses using western blot analysis of viral particles. As shown in Figure 2, all mutant HIV-2 GH123 viruses produced viral particles with processed Gag proteins similar to the wild type virus. These results clearly exclude the possibility that the impaired replication of GH123/K and GH123/R viruses were due to inefficient processing of Gag precursors.

The 118th position of SIVmac239 CA and viral susceptibility to CM TRIM5α

HIV-2, simian immunodeficiency virus isolated from sooty mangabey (SIVsm), and SIVmac have similar genomes [19]. SIVmac239 can replicate in the presence of CM TRIM5α [5] and

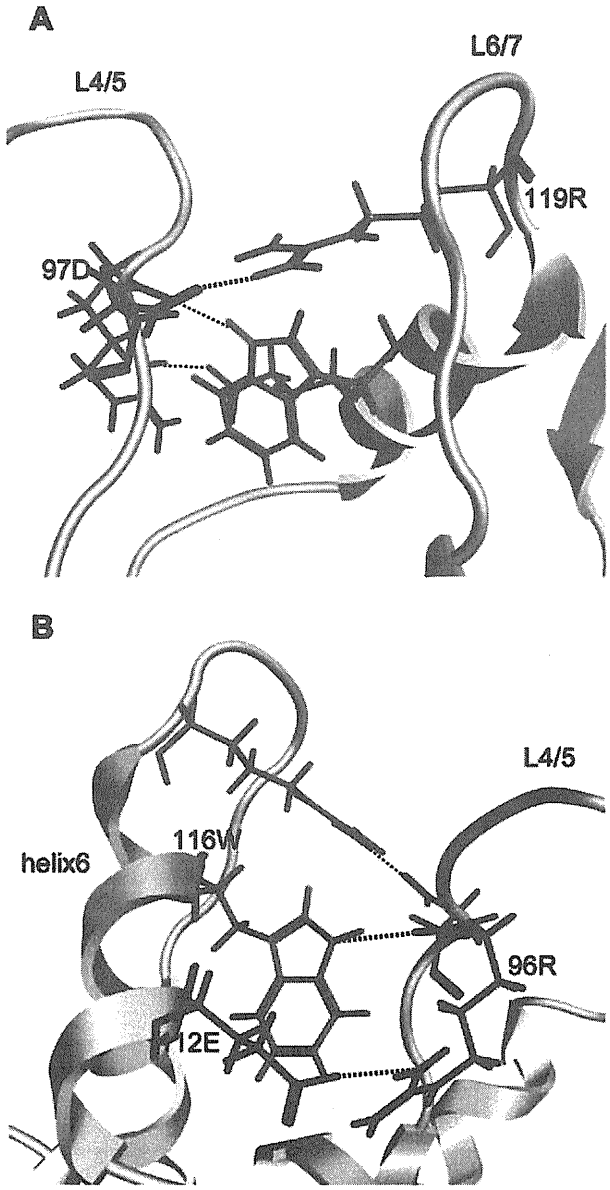

Figure 5. Hydrogen bond formation among L4/5, L6/7 and helix 6 of the HIV-2 CA. Close-up views of averaged structures of the N-terminal domain of the GH123/P CA during 5–20 nanoseconds of MD simulations are shown. Red, blue, purple, orange and green wireframes denote side chains of arginine at the 96th (96R), aspartic acid at the 97th (97D), glutamic acid at the 112th (112E), tryptophan at the 116th (116W) and arginine at the 119th (119R) positions, respectively. Dotted lines indicate hydrogen bonds visualized with MOE 2009. Models from two different angles are shown.
doi:10.1371/journal.pone.0022779.g005

contains Q at the 118th position, which corresponds to the 120th position of the GH123 CA. In our previous study, we reported that mutant SIVmac239 carrying P at the 118th position (SIVmac239/P) became sensitive to CM and human TRIM5αs [20]. In the present study, we examined whether other amino acid residues that conferred resistance (A, G) or sensitivity (valine, V) to CM TRIM5α or abolished viral replicative ability (arginine, R) on a GH123 background showed similar effects on viral sensitivity to CM TRIM5α on an SIVmac239 background.

As shown in Figure 3, CM TRIM5α did not affect the replication of wild type SIVmac239 but inhibited SIVmac239/P, which is in agreement with the results of the previous study [20]. It should be noted, however, that the inhibitory effect of CM TRIM5α on SIVmac239/P was smaller than that on GH123/P, since SIVmac239/P demonstrated some growth even in the presence of CM TRIM5α. Newly generated SIVmac239 carrying alanine (SIVmac239/A) or glycine (SIVmac239/G) at the 118th position were unaffected by CM TRIM5α (Figure 3).

On the other hand, the mutant SIVmac239 carrying valine (SIVmac239/V) was only weakly inhibited by CM TRIM5α (Figure 3) to a lesser degree than the GH123/V. As shown in Figure 1, the inhibitory effect on GH123/V was also smaller than that on GH123/P even on a GH123 background. These results clearly indicate that single amino acid substitutions at the 118th position of the SIVmac239 CA had similar effects to those at the 120th position of GH123, although their impact was smaller in SIVmac239 than in the GH123 CA. Nevertheless, replication of mutant SIVmac239 carrying arginine (SIVmac239/R) was severely impaired, as with GH123/R.

Molecular modeling and molecular dynamics (MD) simulations of the HIV-2 capsid N-terminal domain

The amino acid at position 120 is located in the L6/7 of the N-terminal domain of the CA. To obtain structural insights into the mechanisms by which this amino acid controls viral sensitivity to TRIM5α-mediated restriction, we conducted computer-assisted structural study of the N-terminal domain of the CA. With homology modeling and molecular dynamics (MD) simulation techniques, we constructed a series of initial structural models of the N-terminal half of the CA from CM TRIM5α-sensitive (GH123/P, GH123/F, GH123/H, and GH123/I) and CM TRIM5α-resistant (GH123/Q, GH123/A, GH123/N, and GH123/E) viruses. The initial models were then subjected to the MD simulation to analyze structural dynamics of the N-terminal domain of the CA in water environment. Average structures of individual CA mutants were obtained with 60,000 trajectories during 5–20 nanoseconds of MD simulations.

Comparisons of the average structures revealed that amino acid substitutions at position 120 could significantly influence the overall conformation of the exposed surface of the HIV-2 CA (Figure 4). Notably, the L4/5 of the mutant CAs are classified into two subgroups on the basis of their conformational similarities. These subgroups are primarily coincident with the two phenotypic subgroups based on viral sensitivities to CM TRIM5α, with the exception of mutant GH123/E (Figure 4, cartoon models indicated by gray). TRIM5α-sensitive viruses GH123/P, GH123/F, GH123/H and GH123/I showed almost identical L4/5 conformation (Figure 4, red models), while L4/5 of TRIM5α-resistant viruses GH123/Q, GH123/A and GH123/N were more variable (Figure 4, blue models). To confirm this, we performed additional modeling of TRIM5α-resistant viruses GH123/T and GH123/S. The results showed that L4/5 of GH123/T and GH123/S were also variable (data not shown).

Furthermore, the MD simulation study revealed that the common L4/5 structures of the TRIM5α-sensitive viruses were associated with a reduced probability of hydrogen bond formation between the 97th aspartic acid (D) in L4/5 and the 119th arginine (R) in L6/7 compared with those of TRIM5α-resistant viruses except for GH123/E (Figure 5A and Table 1). We, therefore, hypothesized that the presence of the hydrogen bond between the 97th D in L4/5 and the 119th R in L6/7 disrupted the L4/5 conformation required for recognition by TRIM5α. To examine whether hydrogen bond formation between the 97th D and 119th R indeed affects the viral sensitivity to CM TRIM5α-mediated restriction, we introduced an alanine substitution at the 97th

Table 1. The probability of forming a hydrogen bond between the 97th aspartic acid in L4/5 and the 119th arginine in L6/7 of the CA in 60,000 trajectories during 5–20 nanoseconds of MD simulations and the sensitivity phenotype.

120th amino acid	Frequency of hydrogen bond (%)	Sensitivity to CM TRIM5α
Pro (P)	44.6	Sensitive
Phe (F)	41.5	Sensitive
His (H)	42.99	Sensitive
Ile (I)	0	Sensitive
Ala (A)	64.47	Resistant
Gln (Q)	55.15	Resistant
Asn (N)	55.7	Resistant
Glu (E)	21.27	Resistant
Ser (S)	63.51	Resistant
Thr (T)	51.48	Resistant

doi:10.1371/journal.pone.0022779.t001

position of the TRIM5α-resistant viruses GH123/Q (D97A-GH123/Q) and GH123/A (D97A-GH123/A). The side chain of A at the 97th position would be too small to form a hydrogen bond with the 119th R, which was confirmed by MD simulation study of the D97A CA mutant of GH123/Q (Figure 6). As expected, the D97A substitution conferred moderate sensitivity to CM TRIM5α upon the resistant viruses GH123/Q and GH123/A (Figure 7A and 7B). In the case of TRIM5α-sensitive virus GH123/P, in which the probability of hydrogen bond formation between the 97th D and 119th R was predicted to be low (Table 1), the D97A substitution did not alter the viral senstivity to CM TRIM5α (Figure 7C). These data suggest that the conformation of L4/5, which is influenced by that of L6/7, participates in determining viral sensitivities to CM TRIM5α-mediated restriction. It should be noted, however, that the D97A substitution slightly impaired the replication of GH123/Q and GH123/A, as indicated by the titers of D97A-GH123/Q and D97A-GH123/A, which were apparently lower than those of GH123/Q and GH123/A at day 5 after infection even in the absence of TRIM5α (Figure 7A and 7B).

Although we further tried to disrupt the hydrogen bond formation by introducing an alanine substitution at the 119th position, the resultant mutant viruses did not grow (data not shown). The arginine at the 119th position is highly conserved among different HIV-2 strains and may be essential for virus replication.

In the case of the TRIM5α-resistant virus GH123/E (Figure 4, gray model), however, the conformation of L4/5 was similar to those of CM TRIM5α-sensitive viruses GH123/P, GH123/F, GH123/H and GH123/I (Figure 4, red models). The probability of hydrogen bond formation was also low in GH123/E, unlike that in the other resistant viruses GH123/Q, GH123/A and GH123/N (Table 1). Because GH123/E has a negatively charged amino acid E at the 120th position, we performed additional modeling of the CM TRIM5α-resistant virus with another negatively charged amino acid D (GH123/D). The results showed that the conformation of GH123/D L4/5 was also similar to those of CM TRIM5α-sensitive viruses (data not shown). Consistent with this, the possibility of hydrogen bond formation was low (21.27%) in GH123/D just as in GH123/E. It

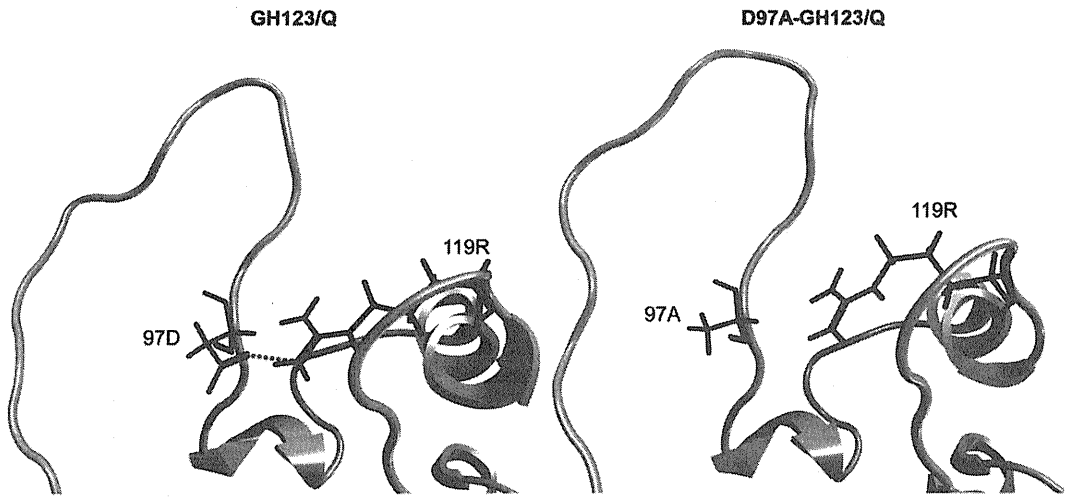

Figure 6. Lack of hydrogen bond formation between the 97th alanine and the 119th arginine of HIV-2 D97A-GH123/Q CA. Close-up views of averaged structures around the L4/5 loop of GH123/Q (left) and D97A-GH123/Q (right) during 5–20 nanoseconds of MD simulations are shown. Red, blue and green wireframes denote side chains of aspartic acid at the 97th (97D), arginine at the 119th (119R), and alanine at the 97th (97A) positions, respectively. A dotted line indicates a hydrogen bond.
doi:10.1371/journal.pone.0022779.g006

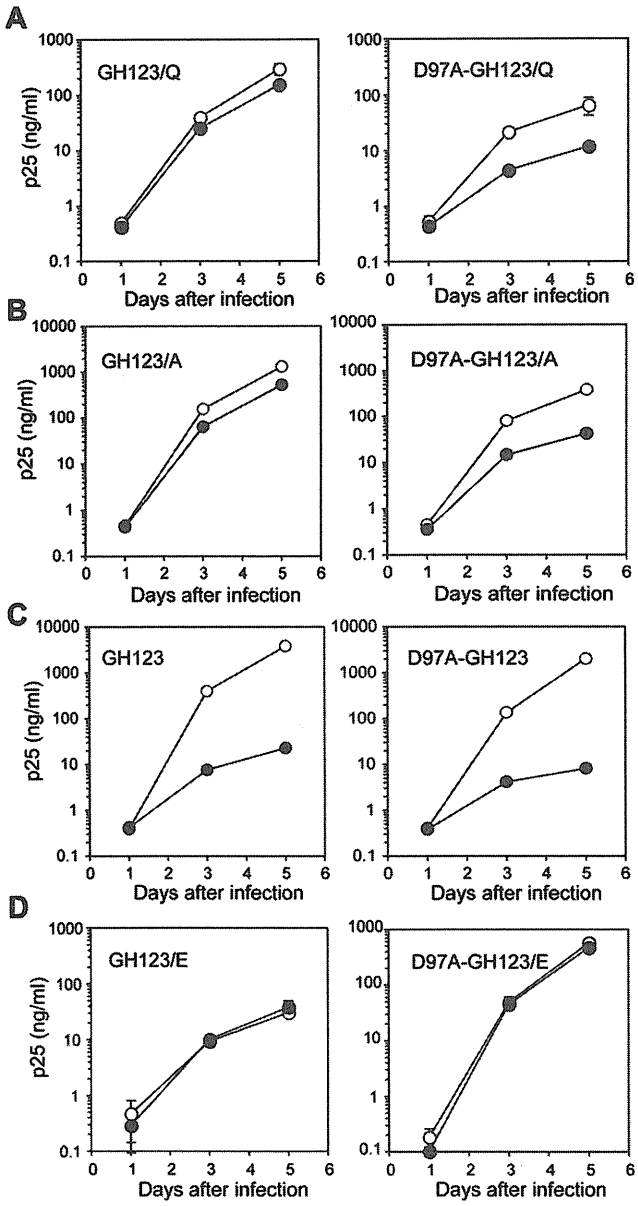

Figure 7. Effects of an aspartic acid-to-alanine substitution at the 97th position of the HIV-2 CA on viral growth in the presence or absence of CM TRIM5α. MT4 cells were infected with CM-TRIM5α-SeV (black circles) or CM-SPRY(–)-SeV (white circles) then superinfected with GH123 mutant viruses. Culture supernatants were periodically assayed for levels of viral capsid. Error bars show actual fluctuations between measurements of capsid in duplicate samples. A representative of three independent experiments is shown.
doi:10.1371/journal.pone.0022779.g007

is possible that the presence of the negative charge at the 120th position prevented access of TRIM5α even though the L4/5 conformation was adequate for TRIM5α recognition. If our modeling of GH123/E L4/5 was correct, disruption of the hydrogen bond between the 97th D and 119th R would have little or no effect on the TRIM5α sensitivity of GH123/E. In fact, the D97A substitution failed to alter the resistant phenotype of GH123/E (Figure 7D), but did unexpectedly compensate the impaired replication of GH123/E (Figure 1B). These results indicate that the effect of D97A substitution depended upon the amino acid residue at the 120th position, and further supported the notion that the L6/7 itself was also involved in CM TRIM5α restriction. Consistent with this, the side chains of amino acid residues at the 120th position were exposed on the surface of the CA (Figure 8).

When these results are considered together, it is likely that the hydrogen bond between the L4/5 and L6/7 modulates the overall structure of the exposed surface of the CA and that both L4/5 and L6/7 are responsible for CA recognition by CM TRIM5α.

Discussion

In the present study, we showed that a hydrogen bond between the 97th D and the 119th R of HIV-2 CA affected viral sensitivity to CM TRIM5α. TRIM5α-sensitive viruses showed a common L4/5 structure, but L6/7 was also important in CA recognition by TRIM5α.

Previously, we proposed that the configuration of HIV-2 CA L6/7 would affect viral sensitivity to CM TRIM5α on the basis of the results of homology modeling of the HIV-2 CA in which the 3-D structure of HIV-1 CA was used as a template [20]. In the present study, however, we performed intensive mutational analysis of the HIV-2 CA followed by more intensive computer-assisted structural analyses using the recently published 3-D structure of the HIV-2 CA and MD simulation, which provide information on structural dynamics of proteins in solution. Results of the present study revealed that alterations in the L4/5 conformation were more strongly associated with viral sensitivity to TRIM5α than those in the L6/7 configuration. Furthermore, the data on the MD simulation study disclosed that a hydrogen bond between the 97th D and the 119th R may be a critical modulator affecting the conformation of L4/5.

In the case of the HIV-1 CA, two hydrogen bonds were reported to form between R at the 229th position of Gag (R229) and E at the 245th position (E245), and between R229 and W at the 249th position (W249) [24]. These three amino acids were also found in the HIV-2 CA; and R229, E245 and W249 of the HIV-1 CA correspond to the 96th R, 112th E and the 116th W of the HIV-2 GH123 CA, respectively (Fig. 5B). The 112th E and 116th W are in the 6th helix of the CA, and the 96th R is adjacent to the 97th D in L4/5. In our HIV-2 CA models, these two hydrogen bonds were observed with a probability of more than 99.9%, regardless of the viral sensitivity to TRIM5α. Therefore, TRIM5α-resistant viruses are likely to have three hydrogen bonds at the base of L4/5, whereas those sensitive to TRIM5α have two hydrogen bonds there. It is possible that reduced structural flexibility of the base of loop causes the upper loop structure to collapse more easily. Thus, the number of the hydrogen bonds may affect the flexibility of the base of L4/5 and the maintenance of the binding surface for TRIM5α, which is formed at least partly by L4/5. As a result, the viral sensitivity to TRIM5α changes.

In the CA sequences of HIV-2 and SIVmac in the Los Alamos Database, the 97th position was always occupied by acidic D or E, and the 119th position was always occupied by R. In the case of HIV-1 or simian immunodeficiency virus isolated from the chimpanzee (SIVcpz), however, the 119th position was occupied by variable amino acid residues, while the 97th position was always occupied by acidic D or E. It should be noted that a hydrogen bond between the 97th and 119th amino acid residues was never observed in the HIV-1 CA (data not shown). Those differences may contribute to the increased sensitivity of HIV-1 to OWM TRIM5α compared with HIV-2 strains.

Although our data showed a clear correlation between viral sensitivity to TRIM5α and the conformation of CA L4/5, there was one exception. The conformation of L4/5 in GH123/E was

almost identical to those of TRIM5α-sensitive viruses, but GH123/E was highly resistant to CM TRIM5α. Furthermore, disruption of the hydrogen bond between the 97th D and the 119th R by substitution of D97A did not alter the resistant phenotype of GH123/E at all. These results suggested that the 120th amino acid residue of the HIV-2 GH123 CA itself is also involved in CM TRIM5α sensitivity independently from the L4/5 conformation. This view was also supported by our present observation that disruption of the hydrogen bond between the 97th D and the 119th R conferred only moderate sensitivity to CM TRIM5α upon another resistant virus GH123/Q (Figure 7).

Replication of GH123/E or GH123/D was slightly impaired (Figure 1B), but this impairment was compensated by the D97A substitution in GH123/E (Figure 7D). On the other hand, replication of GH123/Q was almost comparable to that of GH123 (Figure 1A); but the D97A substitution slightly impaired its replicative capability (Figure 7A). It should be also mentioned here that the viruses with basic residues at the 120th position, GH123/R and GH123/K, scarcely grew (Figure 1B). These results suggest that certain optimum levels of charge are required at the L4/5 and L6/7 for efficient viral replication. At present, it is unclear why those charge differences affect the growth capability of the virus; but it is possible that the charge difference affects the accessibility to unknown host factor(s) involved in uncoating.

HIV-2 closely resembles SIVsm, which is thought to have entered the human population on at least eight separate occasions [19]. Almost all SIV isolates from the Los Alamos Database contain glutamine at the position corresponding to the 119th or 120th position of the HIV-2 CA in the presence of strong OWM TRIM5α pressure. After entry of SIVsm into the human population, which lacks OWM TRIM5α pressure, some viruses were presumably forced to change glutamine to proline by mutating the second nucleotide of the codon. This change may have been driven by specific immune responses against the HIV-2 CA. Similarly, alanine viruses may have evolved from the proline virus after transmission to individuals lacking such responses by changing the first nucleotide of the codon in order to become more resistant to human TRIM5α. Glycine viruses may have further evolved from the alanine virus by changing the second nucleotide of the codon. However, it is unclear why serine, histidine, threonine and leucine viruses have not been identified despite their nearly normal levels of growth. It is possible that certain human immune responses prevented their emergence.

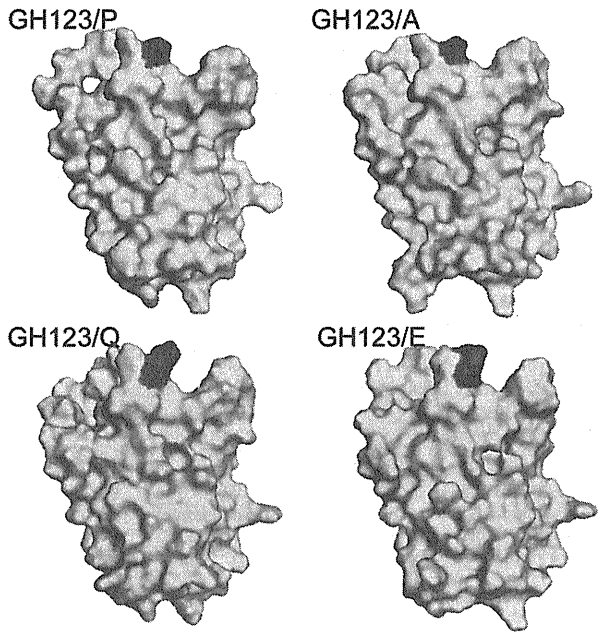

Figure 8. Surface structure of the HIV-2 capsid N-terminal domain. Surface structure of the GH123 and mutant GH123 CAs visualized with PyMOL. Red color indicates the 120th amino acid of the GH123 and mutant GH123 CAs.
doi:10.1371/journal.pone.0022779.g008

In a sharp contrast to CM TRIM5α, Rh TRIM5α could restrict both CM TRIM5α-sensitive and -resistant HIV-2 strains [8]. SIVmac239 is resistant to Rh TRIM5α, but chimeric SIVmac239 with L4/5 of HIV-2 strains GH123 [25] or ROD [21] were efficiently restricted by Rh TRIM5α. Therefore, the L4/5 of HIV-2 CA is also a critical determinant for Rh TRIM5α-mediated restriction. In the present study, we have shown that CM TRIM5α-sensitive HIV-2 viruses have a specific structure in the L4/5 of the CA. However, the 3-D structure of Rh and CM TRIM5α remains unsolved. To elucidate the more detailed molecular mechanism of the interaction between TRIM5α and the CA, structural information about TRIM5α is essential. A docking study based on such information is likely to shed light on the antiviral mechanism of TRIM5α.

In summary, we showed that a hydrogen bond between the 97th D and the 119th R of HIV-2 CA affected viral sensitivity to CM TRIM5α and that both L4/5 and L6/7 are responsible for CA recognition by CM TRIM5α.

Methods

Cell cultures

293T cells were maintained in Dulbecco's Modified Eagle medium, and HeLa cells were maintained in Minimum Essential Medium. The human T-cell line MT4 was maintained in RPMI medium. All media were supplemented with 10% fetal bovine serum and 1% penicillin-streptomycin.

Plasmid construction

Mutant HIV-2 GH123 or SIVmac239 viruses were generated by site-directed mutagenesis. Infectious viruses were prepared by transfection of 293T cells with resultant proviral DNA clones. The viral titer was determined by measuring p25 or p27 with a RetroTek antigen ELISA kit (ZeptoMetrix, Buffalo, NY).

Construction of recombinant Sendai viruses (SeV) expressing C-terminally HA-tagged CM TRIM5α (CM-TRIM5α-SeV) and CM-TRIM5α lacking the PRYSPRY domain (CM-SPRY(–)-SeV) were described previously [5,20].

Viral infection

MT4 cells (1×10^5) were infected with SeV expressing each of the TRIM5αs at a multiplicity of infection of 10 plaque-forming units per cell and incubated at 37°C for 9 h. Cells were then superinfected with 20 ng of p25 of HIV-2 GH123 derivatives or with 40 ng of p27 SIVmac239 derivatives. The culture supernatants were collected periodically, and the level of p25 or p27 was measured with a RetroTek antigen ELISA kit (ZeptoMetrix).

Viral particle purification and western blotting

The culture supernatant of 293T cells transfected with plasmids encoding HIV-2 GH123 and GH123 mutants were clarified by low-speed centrifugation. The resultant supernatants (10 ml) were layered onto a 2 ml cushion of 20% sucrose and centrifuged at 35,000 rpm for 2 h at 4°C in a Beckman SW41 rotor. Pelleted viral particles were resuspended in PBS. Lysates were normalized

based on p25 antigen concentrations and were analyzed by western blotting with the SIV-infected monkey serum.

Molecular modeling and MD simulation

We used MD simulations [26] to analyze structural dynamics of the HIV-2 CA N-terminal domain. First, initial CA structures for MD simulation were constructed by homology modeling [27] using the Molecular Operating Environment, MOE 2008.1002 (Chemical Computing Group Inc., Montreal, Quebec, Canada) as described [20,28]. We used the high-resolution crystal structure of the HIV-2 CA N-terminal domain at a resolution of 1.25 Å (PDB code: 2WLV [29]) as the modeling template. Structural dynamics of these HIV-2 CA models in water environment were analyzed using MD simulations with the SANDER module in the AMBER 9 program package [30] and the AMBER99SB force field [31] with the TIP3P water model. Bond lengths involving hydrogen were constrained with SHAKE [32] and the time step for all MD simulations was set to 2 fs. After heating calculations for 20 ps to 310 K using the NVT ensemble, the simulations were executed using the NPT ensemble at 1 atm and at 310 K for 20 ns. Hydration analyses were performed using the ptraj module in AMBER. A maximum cutoff angle of 120.0° and cutoff length of 3.5 Å were used in hydrogen bond definitions. The surface structure of CA is visualized with PyMOL 1.2r1 (The PyMOL Molecular Graphics System, http://pymol.sourceforge.net/).

Acknowledgments

We thank Dr. A. Kuroishi, Dr. S. Nakamura and Dr. T. Yasunaga for helpful discussions and Ms. S. Bando and Ms. N. Teramoto for assistance.

Author Contributions

Conceived and designed the experiments: TS HS EEN. Performed the experiments: TM MY KK EEN. Analyzed the data: TS HS EEN. Wrote the paper: TM HS TS EEN.

References

1. Stremlau M, Owens CM, Perron MJ, Kiessling M, Autissier P, et al. (2004) The cytoplasmic body component TRIM5alpha restricts HIV-1 infection in Old World monkeys. Nature 427: 848–853.
2. Reymond A, Meroni G, Fantozzi A, Merla G, Cairo S, et al. (2001) The tripartite motif family identifies cell compartments. Embo J 20: 2140–2151.
3. Perez-Caballero D, Hatziioannou T, Yang A, Cowan S, Bieniasz PD (2005) Human tripartite motif 5alpha domains responsible for retrovirus restriction activity and specificity. J Virol 79: 8969–8978.
4. Sawyer SL, Wu LI, Emerman M, Malik HS (2005) Positive selection of primate TRIM5alpha identifies a critical species-specific retroviral restriction domain. Proc Natl Acad Sci U S A 102: 2832–2837.
5. Nakayama EE, Miyoshi H, Nagai Y, Shioda T (2005) A specific region of 37 amino acid residues in the SPRY (B30.2) domain of African green monkey TRIM5alpha determines species-specific restriction of simian immunodeficiency virus SIVmac infection. J Virol 79: 8870–8877.
6. Ohkura S, Yap MW, Sheldon T, Stoye JP (2006) All three variable regions of the TRIM5alpha B30.2 domain can contribute to the specificity of retrovirus restriction. J Virol 80: 8554–8565.
7. Perron MJ, Stremlau M, Sodroski J (2006) Two surface-exposed elements of the B30.2/SPRY domain as potency determinants of N-tropic murine leukemia virus restriction by human TRIM5alpha. J Virol 80: 5631–5636.
8. Kono K, Song H, Shingai Y, Shioda T, Nakayama EE (2008) Comparison of anti-viral activity of rhesus monkey and cynomolgus monkey TRIM5alphas against human immunodeficiency virus type 2 infection. Virology 373: 447–456.
9. Kono K, Bozek K, Domingues FS, Shioda T, Nakayama EE (2009) Impact of a single amino acid in the variable region 2 of the Old World monkey TRIM5alpha SPRY (B30.2) domain on anti-human immunodeficiency virus type 2 activity. Virology 388: 160–168.
10. Yap MW, Nisole S, Stoye JP (2005) A single amino acid change in the SPRY domain of human Trim5alpha leads to HIV-1 restriction. Curr Biol 15: 73–78.
11. Stremlau M, Perron M, Welikala S, Sodroski J (2005) Species-specific variation in the B30.2(SPRY) domain of TRIM5alpha determines the potency of human immunodeficiency virus restriction. J Virol 79: 3139–3145.
12. Hatziioannou T, Perez-Caballero D, Yang A, Cowan S, Bieniasz PD (2004) Retrovirus resistance factors Ref1 and Lv1 are species-specific variants of TRIM5alpha. Proc Natl Acad Sci U S A 101: 10774–10779.
13. Sebastian S, Luban J (2005) TRIM5alpha selectively binds a restriction-sensitive retroviral capsid. Retrovirology 2: 40.
14. Stremlau M, Perron M, Lee M, Li Y, Song B, et al. (2006) Specific recognition and accelerated uncoating of retroviral capsids by the TRIM5alpha restriction factor. Proc Natl Acad Sci U S A 103: 5514–5519.
15. Rold CJ, Aiken C (2008) Proteasomal degradation of TRIM5alpha during retrovirus restriction. PLoS Pathog 4: e1000074.
16. Anderson JL, Campbell EM, Wu X, Vandegraaff N, Engelman A, et al. (2006) Proteasome inhibition reveals that a functional preintegration complex intermediate can be generated during restriction by diverse TRIM5 proteins. J Virol 80: 9754–9760.
17. Wu X, Anderson JL, Campbell EM, Joseph AM, Hope TJ (2006) Proteasome inhibitors uncouple rhesus TRIM5alpha restriction of HIV-1 reverse transcription and infection. Proc Natl Acad Sci U S A 103: 7465–7470.
18. Maegawa H, Miyamoto T, Sakuragi J, Shioda T, Nakayama EE (2010) Contribution of RING domain to retrovirus restriction by TRIM5alpha depends on combination of host and virus. Virology 399: 212–220.
19. Hahn BH, Shaw GM, De Cock KM, Sharp PM (2000) AIDS as a zoonosis: scientific and public health implications. Science 287: 607–614.
20. Song H, Nakayama EE, Yokoyama M, Sato H, Levy JA, et al. (2007) A single amino acid of the human immunodeficiency virus type 2 capsid affects its replication in the presence of cynomolgus monkey and human TRIM5alphas. J Virol 81: 7280–7285.
21. Ylinen LM, Keckesova Z, Wilson SJ, Ranasinghe S, Towers GJ (2005) Differential restriction of human immunodeficiency virus type 2 and simian immunodeficiency virus SIVmac by TRIM5alpha alleles. J Virol 79: 11580–11587.
22. Onyango CO, Leligdowicz A, Yokoyama M, Sato H, Song H, et al. (2010) HIV-2 capsids distinguish high and low virus load patients in a West African community cohort. Vaccine 28S2: B60–B67.
23. Kuroishi A, Saito A, Shingai Y, Shioda T, Nomaguchi M, et al. (2009) Modification of a loop sequence between alpha-helices 6 and 7 of virus capsid (CA) protein in a human immunodeficiency virus type 1 (HIV-1) derivative that has simian immunodeficiency virus (SIVmac239) vif and CA alpha-helices 4 and 5 loop improves replication in cynomolgus monkey cells. Retrovirology 6: 70.
24. Martinez-Picado J, Prado JG, Fry EE, Pfafferott K, Leslie A, et al. (2006) Fitness cost of escape mutations in p24 Gag in association with control of human immunodeficiency virus type 1. J Virol 80: 3617–3623.
25. Kono K, Song H, Yokoyama M, Sato H, Shioda T, et al. (2010) Multiple sites in the N-terminal half of simian immunodeficiency virus capsid protein contribute to evasion from rhesus monkey TRIM5alpha-mediated restriction. Retrovirology 7: 72.
26. Dodson GG, Lane DP, Verma CS (2008) Molecular simulations of protein dynamics: new windows on mechanisms in biology. EMBO Rep 9: 144–150.
27. Baker D, Sali A (2001) Protein structure prediction and structural genomics. Science 294: 93–96.
28. Shirakawa K, Takaori-Kondo A, Yokoyama M, Izumi T, Matsui M, et al. (2008) Phosphorylation of APOBEC3G by protein kinase A regulates its interaction with HIV-1 Vif. Nat Struct Mol Biol 15: 1184–1191.
29. Price AJ, Marzetta F, Lammers M, Ylinen LM, Schaller T, et al. (2009) Active site remodeling switches HIV specificity of antiretroviral TRIMCyp. Nat Struct Mol Biol 16: 1036–1042.
30. Case DA, Darden TA, Cheatham TEI, Simmerling CL, Wang J, et al. (2006) AMBER 9, University of California, San Francisco.
31. Hornak V, Abel R, Okur A, Strockbine B, Roitberg A, et al. (2006) Comparison of multiple Amber force fields and development of improved protein backbone parameters. Proteins 65: 712–725.
32. Ryckaert JP, Ciccotti G, Berendsen HJC (1977) Numerical integration of the cartesian equations of motion of a system with constraints: Molecular dynamics of n-alkanes. J Comput Phys 23: 327–341.

FEBS Letters 585 (2011) 3372–3377

ELSEVIER

FEBS Letters

journal homepage: www.FEBSLetters.org

Identification of amino acid residues in HIV-1 reverse transcriptase that are critical for the proteolytic processing of Gag–Pol precursors

Hironori Nishitsuji [a,*], Masaru Yokoyama [c], Hironori Sato [c], Suguru Yamauchi [a], Hiroshi Takaku [a,b,*]

[a] Department of Life and Environmental Sciences, Chiba Institute of Technology, 2-17-1 Tsudanuma, Narashino, Chiba 275-0016, Japan
[b] High Technology Research Center, Chiba Institute of Technology, 2-17-1 Tsudanuma, Narashino, Chiba 275-0016, Japan
[c] Pathogen Genomics Center, National Institute of Infectious Diseases, 4-7-1 Gakuen, Musashi Murayama-shi, Tokyo 208-0011, Japan

ARTICLE INFO

Article history:
Received 1 July 2011
Revised 22 September 2011
Accepted 23 September 2011
Available online 12 October 2011

Edited by Ivan Sadowski

Keywords:
Human immunodeficiency virus type 1
Reverse transcriptase
Gag–Pol
Processing

ABSTRACT

The efficient processing of human immunodeficiency virus type 1 Gag–Pol requires not only protease activity but also specific reverse transcriptase (RT) and integrase sequences. However, the critical amino acid residues of the HIV-1 Pol gene involved in protease-mediated Gag–Pol processing have not been precisely defined. Here, we found that the substitution of Thr-128 or Tyr-146 with Ala markedly impaired the proteolytic processing of the MA/CA, p66/p51 and RT/IN sites but did not affect the normal processing of other sites. Moreover, a Thr-128 or Tyr-146 mutation in RT abolished RT dimerization in vitro. These results suggest that Thr-128 and Tyr-146 within the RT region play important roles in protease-mediated Gag–Pol processing.

Structured summary of protein interactions:
RT and **RT** physically interact by cross-linking study (View interaction: 1, 2, 3).
CK2 alpha phosphorylates RT by protein kinase assay (View interaction).

1. Introduction

The human immunodeficiency virus type 1 (HIV-1) Gag–Pol is normally translated by a −1 ribosomal frameshift event occurring at a frequency of approximately 5% during Gag translation, resulting in a 1:20 ratio of synthesized Gag–Pol to Pr55-Gag [1]. The incorporation of Gag–Pol into virus particles requires its interaction with Pr55-Gag [2]. The processing of Gag–Pol is accomplished by viral protease activation during Gag–Pol/Gag–Pol interactions or Gag–Pol multimerization [3]. The proteolytic processing of Gag follows a sequential cascade of events that is kinetically controlled by differential rates of processing at each of the five cleavage sites in Gag [4,5]. Protease-mediated Gag–Pol processing requires the protease as well as domains upstream or downstream of the protease region, such as the reverse transcriptase (RT) and integrase (IN) domains. Mutants with an IN-domain deletion form markedly impaired viral particles due to the impairment of normal protease activity [6]. Mature HIV-1 RT is a heterodimer with two subunits, p66 and p51. The p51 subunit is derived from p66 by the proteolytic removal of the C-terminal RNaseH domain. RT–RT interactions may play important roles in protease activation by promoting Gag–Pol multimerization. RT inhibitors enhance RT dimerization in vitro, resulting in increased protease-specific cleavage of Pr55-Gag and Gag–Pol [7]. However, the deletion of the RT region leads to a marked reduction in protease activation and particle maturation [8]. The critical amino acid residues of the HIV-1 RT that contribute to protease-mediated Gag–Pol processing are not yet known.

In this study, we identified the HIV-1 RT amino acid residues critical for Gag–Pol processing through the analysis of RT phosphorylation. The substitution of Thr-128 and Tyr-146 with Ala severely impaired viral replication, due to defects in proteolytic processing at the MA/CA, p66/p51, and RT/IN sites.

2. Materials and methods

2.1. Plasmids

Details of the plasmid constructs used in this study are provided in the Supplementary materials and methods.

2.2. Virus infection

For infection, 293T cells were co-transfected with 0.1 μg of pMD.G-VSV-G and 0.1 μg of pNL43lucΔenv or pNL43lucΔenv

Abbreviations: HIV-1, human immunodeficiency virus type 1; RT, reverse transcriptase; DTSSP, 3,3′-dithiobis(sulfosuccinimidylpropionate); PR, protease

* Corresponding authors. Address: Department of Life and Environmental Sciences, Chiba Institute of Technology, 2-17-1 Tsudanuma, Narashino, Chiba 275-0016, Japan (H. Takaku). Fax: +81 47 478 0407.
E-mail addresses: hironori.nishitsuji@it-chiba.ac.jp (H. Nishitsuji), hiroshi.takaku@it-chiba.ac.jp (H. Takaku).

0014-5793/$36.00 © 2011 Federation of European Biochemical Societies. Published by Elsevier B.V. All rights reserved.
doi:10.1016/j.febslet.2011.09.034

containing an RT mutation of interest. At 48 h post-transfection, the culture supernatants were harvested and filtered through 0.45-μm filters. 293T cells were infected with pseudotyped viruses (corresponding to 20 ng of p24). At 24 h postinfection, the cells were harvested and lysed with 300 μl of cell-lysis buffer. An aliquot (10 μl) of each lysate was then subjected to a luciferase assay.

2.3. Preparation of virions

Details are given in the Supplementary materials and methods.

2.4. Preparation of anti-RT sera

Details of anti-RT sera used in this study are given in the Supplementary materials and methods.

2.5. Crosslinking

Crosslinking was performed as previously described [9].

2.6. Phosphorylation assay

Details are given in the Supplementary materials and methods.

3. Results

3.1. Infectivity of RT-mutant viruses

Recent studies have indicated that the phosphorylation of HIV-1 RT might play an important role in HIV-1 replication [10–11]. To evaluate the role of the putatively phosphorylated RT, we predicted the phosphorylation site(s) of RT using the Scansite 2.0 program [12] and generated single-amino-acid Ala substitutions for the Ser, Thr, and Tyr residues that are conserved among HIV-1 and simian immunodeficiency virus strains. We examined the effect of each mutation on viral replication using a single-round infection system (Fig. 1A). In this study, infection with the S156A mutant led to slightly diminished luciferase activity (approximately 75% of the WT level). Similarly, the single amino acid substitutions of Thr to Ala at position 27 (T27A) and Ser to Ala at position 68 or 105 (S68A and S105A, respectively) resulted in lower levels of luciferase activity (60–65% of the WT level). The infectivity of the RT mutant virus possessing a T58A or T107A mutation significantly decreased to 5–10% of the WT-virus level. The introduction of the T131A, T216A, Y318A, T128A, Y146A or Y183A mutations completely abolished viral infectivity.

To evaluate whether HIV-1 RT mutations affect RT activity, we used the Vpr-p66-WT fusion protein (Fig. 1B), which can be efficiently incorporated into virions [13–14]. The infectivity of T58A, T216A and Y318A was partially restored from 27% to 55% of the WT infectivity by complementation with Vpr-p66-WT-V5 (Fig. 1C). In this complementation, Vpr-p66-WT-V5 was efficiently packaged and processed (Fig. 1E). The T107A mutant was not complemented by Vpr-p66-WT-V5. In addition, the level of RNaseH-V5 in T107A was significantly decreased compared with the WT virion, although the Vpr-p66-WT-V5 and p66-WT-V5 levels in the T107A mutant were similar to WT levels. Moreover, the T131A, and Y183A mutations, which resulted in lower levels of p66-WT-V5 and RNaseH-V5, were not complemented despite the presence of Vpr-p66-WT-V5 (1.3–3.5% of the WT level). In the T128A and Y146A mutants, the majority of Vpr-p66-WT-V5 in the virions remained in the form of unprocessed fusion proteins, and these mutants exhibited defective viral replication (0.5–3.1% of the WT level). To further examine whether incorporating Gag–Pol-WT *in trans* restores the infectivity of the mutant viruses, Gag–Pol-complemented viruses were analyzed for infectivity using a luciferase assay (Fig. 1D). With the exception of Y183A, mutant virus infectivity was partially rescued (26–75% of WT level) by this complementation. Of particular note, a Y183A mutation incorporated into the WT Gag–Pol did not complement infectivity. This result was due to the p66-Y183A mutation displaying some inhibitory potency, as indicated by Vpr-p66-Y183A packaging into the WT virion (data not shown). We concluded that the replication defects associated with the T58A, T216A and Y318A mutants were due primarily to the disruption of RT activity, whereas Thr-107, Thr-128, Thr-131, Tyr-146, and Tyr-183 may be involved in Gag–Pol functions in HIV-1 replication.

3.2. Mutations of Thr-128 and Tyr-146 in RT abolish Gag–Pol processing

To study whether the mutant RTs in the viral particles were present in the p66 and p51 form of the RT, we used anti-RT serum to detect virus-associated mutant RTs (Fig. 2A). The T128A, T131A and Y146A mutations were not found in the p51 form of the RT. Although all of the mutant RTs in the viral particles were detected in the p66 form, T128A, T131A, Y146A, and Y318A mutants had slightly reduced levels of the p66 form relative to the WT. These mutants may be subject to PR-mediated degradation [15].

We next examined the profiles of particle-associated viral proteins to identify possible Gag–Pol processing defects in these mutants. The majority of the Gag-related proteins in the T128A and Y146A mutant virions remained as unprocessed Pr55-Gag (Fig. 2B). The defective Gag-processing phenotype of the T128A and Y146A virions was apparent from the altered ratio of the Pr55-Gag and p24 forms of the CA protein (Fig. 2C). Moreover, the protein levels of HIV-1 protease and integrase were significantly reduced in the T128A and Y148A virions (Fig. 2D and E). Thus, a single amino-acid substitution for Thr-128 or Tyr-148 in the RT appeared to be responsible for the observed effects on Gag–Pol processing.

3.3. Proteolytic cleavage of Gag–Pol was severely impaired at the MA/CA and RT/IN sites in T128A and Y146A virions

To determine the defective sites of Gag–Pol processing in detail, we incorporated several truncated Gag or Pol domains into HIV-1 virions *in trans* as fusion partners of Vpr (Fig. S1A). The proportion of the processed products cleaved at the MA/CA and RT/IN sites was significantly reduced in T128A and Y146A mutants (Fig. S1B and F). In contrast, the cleavage patterns for the SP1/NC, NC/SP2, and SP2/P6 sites in T128A and Y146A mutants were similar to those of the WT (Fig. S1C, D and E). These results suggest that protease-mediated Gag–Pol processing in T128A and Y146A virions was partially affected, but these mutants retained protease activity.

3.4. HIV-1 Gag–Pol processing is dependent on RT dimerization

To determine whether RT dimerization was required for Gag–Pol processing, we used DTSSP (3,3′-dithiobis(sulfosuccinimidylpropionate)) to cross-link protein complexes present in the RT-V5-expressing 293T cells. Only RT monomers were detected in the non-cross-linked samples, with the exception of the Y146A mutant. The addition of 0.2 mM DTSSP yielded cross-linked complexes of RT homodimers when RT-WT-V5 was expressed in 293T cells (Fig. 3). A T131A mutation slightly reduced the level of RT homodimers in the presence of DTSSP compared with the wild type. In contrast, an abnormal pattern was observed in the Y146A mutant in the absence or presence of DTSSP, suggesting that Y146A induced improper folding. Moreover, a T128A mutation resulted in very low levels of the dimer under the same experimental conditions. T58A, Y183A and T216A mutations, which resulted in normal Gag–Pol, retained RT dimerization in the presence of DTSSP. These results suggest that

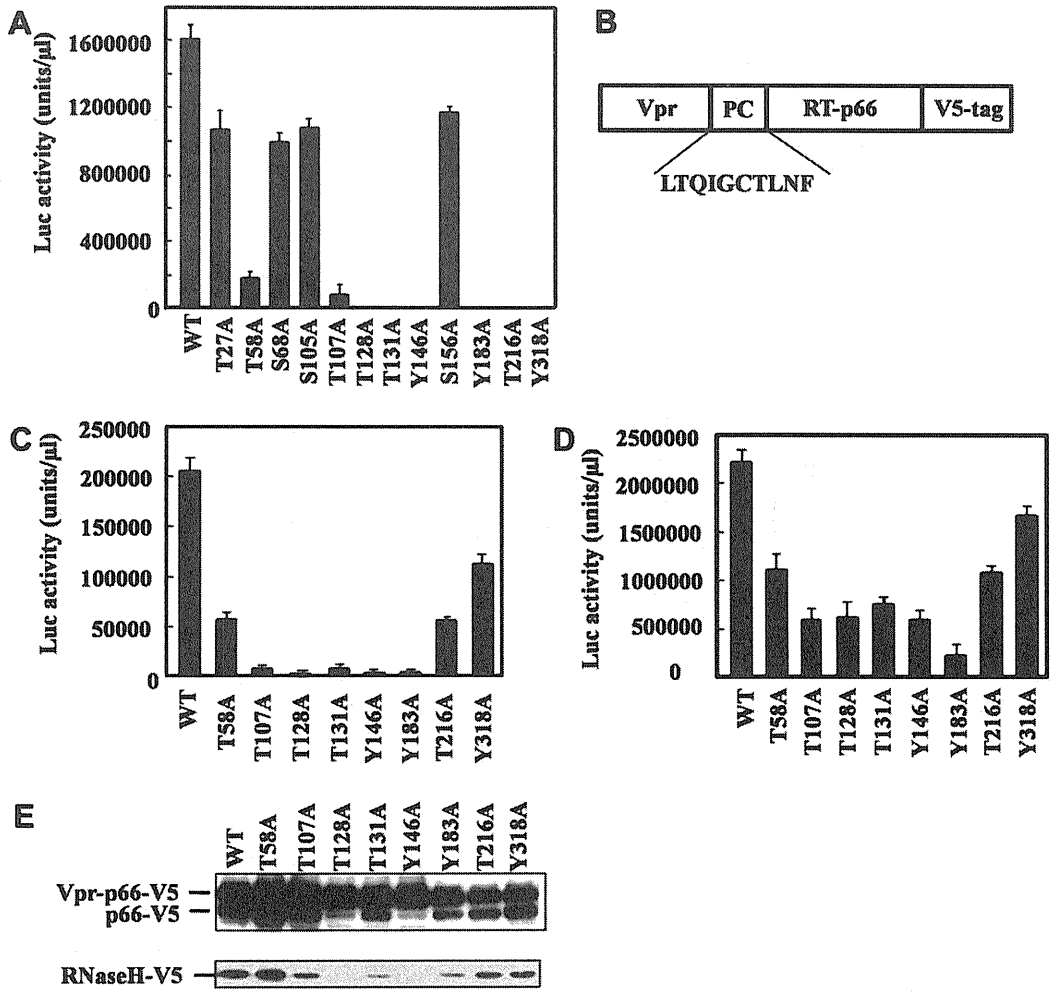

Fig. 1. Infectivity of HIV-1 RT mutants. (A) 293T cells were transfected with 0.1 μg of pMD.G-VSV-G and 0.1 μg of pNL43lucΔenv containing the indicated RT mutations. The 293T cells were infected by pseudoviruses isolated from cell culture supernatants. The luciferase activity in the infected cells was measured 24 h postinfection. (B) An illustration of the Vpr-p66-WT fusion protein including ten amino acids of the protease cleavage sequence at the Vpr-RT junction. (C, D) The 293T cells were transfected with 0.1 μg of wild type (WT) or each RT mutant pNL43lucΔenv, 0.1 μg of pMD.G-VSV-G and 0.2 μg of pVpr-p66-WT-V5 (C) or pMDL-g/p-RRE (D). At 48 h post-transfection, the 293T cells were infected with the indicated pseudotyped viruses. Luciferase activities in the infected cells were measured 24 h postinfection. (E) Culture supernatants in Fig. 1C were collected and subjected to Western immunoblot analysis using an anti-V5 antibody.

RT dimerization may affect Gag–Pol processing. However, the possibility that the T128A and Y146A mutations significantly change the conformation of Gag–Pol precursor, decreasing the accessibility of the targets, cannot be excluded.

3.5. Detection of RT phoshorylation

Harada et al. have reported that HIV RT can be phosphorylated in vitro by casein kinase 2 (CK2-alpha) [16]. We used Phos-tag SDS–PAGE to determine whether CK2-alpha could phosphorylate HIV-1 RT. A phos-tag binds to two Mn^{2+} ions and acts as a phosphate-binding molecule [17]. This complex is used for phosphate affinity SDS–PAGE, in which a mobility shift can be observed with phosphorylated proteins. Recombinant His-RT was incubated with recombinant CK2-alpha in the presence of ATP. As shown in Fig. 4A, a shifted band of recombinant His-RT-WT was observed in the presence of recombinant CK2-alpha in a dose-dependent manner. We next examined the phosphorylation of mutant RT. The phosphorylation levels of His-RT-T128A were similar to wild-type RT (Fig. 4B). In the case of the His-RT-Y146A mutants, the phosphorylation levels were slightly reduced compared with wild-type levels. Moreover, both the T128A and Y146A mutations in recombinant His-RT severely decreased the phosphorylation levels. However, a shifted band corresponding to phosphorylated His-RT-T128A-Y146A could be detected by using a large amount of recombinant His-RT-T128A-Y146A in an in vitro kinase assay (Fig. 4C). To further confirm the phosphorylation of HA-RT-wild and its RT mutants in vivo, HA-tagged RT or its mutants were expressed in 293T cells and the cell lysates were immunoprecipitated with anti-HA antibody. The immune complex was analyzed by Phos-tag, a probe used to detect phosphorylated proteins (Fig. 4D). Wild-type RT was phosphorylated in vivo. However, RT-T128A-Y146A significantly reduced the phosphorylation levels. These results suggest that the T128 and Y146 residues, but not the RT phosphorylation sites, which demonstrated a defect in RT dimerization, affected RT phosphorylation. RT phosphorylation may be required for its dimerization.

4. Discussion

Dunn et al. have reported that an L264S or E302Q mutation in RT rendered the protein susceptible to degradation by PR within virions [15]. In contrast, we identified here the critical amino acid residues (T128 and Y146) that specifically affected RT dimerization but had little effect on the stability of RT. To obtain structural insights into the findings, we constructed a 3-D model of p51/p66 heterodimer of the wild-type (NL43) RT. The model shows that